Quaternary Science Reviews 301 (2023) 107908

Contents lists available at ScienceDirect

Quaternary Science Reviews

journal homepage: www.elsevier.com/locate/quascirev

Revised age and stratigraphy of the classic *Homo erectus*-bearing succession at Trinil (Java, Indonesia)

Sander L. Hilgen [a, d, *], Eduard Pop [a, e], Shinatria Adhityatama [b, f], Tom A. Veldkamp [g], Harold W.K. Berghuis [e], Indra Sutisna [h], Dida Yurnaldi [h], Guillaume Dupont-Nivet [i, j], Tony Reimann [k, l], Norbert Nowaczyk [m], Klaudia F. Kuiper [d], Wout Krijgsman [n], Hubert B. Vonhof [o], Dian Rahayu Ekowati [b], Gerrit Alink [e], Ni Luh Gde Dyah Mega Hafsari [c], Olafianto Drespriputra [p], Alexander Verpoorte [e], Remco Bos [n], Truman Simanjuntak [b], Bagyo Prasetyo [b, 1], Josephine C.A. Joordens [a, e, q]

[a] *Naturalis Biodiversity Center, P.O. Box 9517, Leiden, the Netherlands*
[b] *Pusat Penelitian Arkeologi Nasional (PUSLIT ARKENAS), Jl. Condet Pejaten No.4, Jakarta, 12510, Indonesia*[2]
[c] *Pusat Riset Arkeologi, Lingkungan, Maritim, Dan Budaya Berkelanjutan, Badan Riset Inovasi Nasional (BRIN), Jakarta, Indonesia*
[d] *Faculty of Science, Vrije Universiteit, de Boelelaan 1085, 1081HV, Amsterdam, the Netherlands*
[e] *Faculty of Archaeology, Leiden University, P.O. Box 9514, Leiden, the Netherlands*
[f] *School of Humanities, Languages and Social Science, Griffith University, Gold Coast, Queensland, Australia*
[g] *Faculty ITC, University of Twente, P.O. Box 217, 7500 AE, Enschede, the Netherlands*
[h] *Geological Museum, Jl. Diponegoro 57 Bandung, Jawa Barat, 40122, Bandung, Indonesia*
[i] *Institute of Geosciences, Potsdam University, Potsdam, Germany*
[j] *Géosciences Rennes, UMR CNRS 6118, Université de Rennes, Rennes, France*
[k] *Soil Geography and Landscape Group and Netherlands Centre for Luminescence Dating, Environmental Sciences, Wageningen University, Wageningen, the Netherlands*
[l] *Universität zu Köln, Albertus-Magnus-Platz, 50923, Köln, Germany*
[m] *GeoForschungsZentrum (GFZ) Helmholtz Centrum, Telegrafenberg, 14473, Potsdam, Germany*
[n] *Universiteit Utrecht, Heidelberglaan 8, 3584 CS, Utrecht, the Netherlands*
[o] *Max Planck Institute for Chemistry, Hahn-Meitner-Weg 1, 55128, Mainz, Germany*
[p] *Muséum National D'Histoire Naturelle, 57 Rue Cuvier, 75005, Paris, France*
[q] *Faculty of Science and Engineering, Maastricht University, Paul-Henri Spaaklaan 1, 6229 EN, Maastricht, the Netherlands*

ARTICLE INFO

Article history:
Received 3 October 2022
Received in revised form
1 December 2022
Accepted 2 December 2022
Available online xxx

Handling Editor: Dr Donatella Magri

Keywords:
Pleistocene
Hominin evolution
Biostratigraphy
$^{40}Ar/^{39}Ar$
Luminescence dating
Paleomagnetism

ABSTRACT

Obtaining accurate age control for fossils found on Java (Indonesia) has been and remains challenging due to geochronologic and stratigraphic uncertainties. In the 1890s, Dubois excavated numerous faunal fossils—including the first remains of *Homo erectus*—in sediments exposed along the Solo River at Trinil. Since then, various, and often contradictory age estimates have been proposed for the Trinil site and its fossils. However, the age of the fossil-bearing layers and the fossil assemblage remains inconclusive. This study constructs a chronostratigraphic framework for the Trinil site by documenting new stratigraphic sections and test pits, and by applying $^{40}Ar/^{39}Ar$, paleomagnetic, and luminescence ($pIRIR_{290}$) dating methods. Our study identifies two distinct, highly fossiliferous channel fills at the Trinil site. The stratigraphically lower Bone-Bearing Channel 1 (BBC-1) dates to 830–773 ka, while Bone-Bearing Channel 2 (BBC-2) is substantially younger with a maximum age of 450 ± 110 ka and an inferred minimum age of 430 ± 50 ka. Furthermore, significantly younger T2 terrace deposits are present at similar low elevations as BBC-1 and BBC-2. Our results demonstrate the presence of Early and Middle Pleistocene, and potentially even late Middle to Late Pleistocene fossiliferous sediments within the historical excavation area, suggesting that Dubois excavated fossils from at least three highly fossiliferous units with different ages. Moreover, evidence for reworking suggests that material found in the fossil-rich

* Corresponding author. Naturalis Biodiversity Center, P.O. Box 9517, Leiden, the Netherlands. (S.L. Hilgen).
E-mail address: sander.hilgen@naturalis.nl (S. L. Hilgen).
[1] Deceased.
[2] As of early 2022, the institute PUSLIT ARKENAS no longer exists and is replaced by [c].

https://doi.org/10.1016/j.quascirev.2022.107908

strata may originate from older deposits, introducing an additional source of temporal heterogeneity in the Trinil fossil assemblage. This challenges the current assumption that the Trinil H.K. fauna –which includes *Homo erectus*-is a homogeneous biostratigraphic unit. Furthermore, this scenario might explain why the Trinil skullcap collected by Dubois is tentatively grouped with *Homo erectus* fossils from Early Pleistocene sediments at Sangiran, while Trinil Femur I shares affinities with hominin fossils of Late Pleistocene age.

1. Introduction

In his search for fossil evidence of a transitional form between apes and humans, Eugène Dubois conducted large-scale excavations along the Solo River near the village of Trinil, East Java, Indonesia between 1891 and 1900 (Fig. 1; Theunissen, 1981; Vos and Aziz, 1989). From the fossil-rich deposits along the riverbanks, thousands of vertebrate remains were recovered, including a primate femur (Femur I), a skullcap, two molars, and later a premolar. Dubois considered these fossils to be of the same species that he called *Pithecanthropus erectus* (Dubois, 1894, 1895, 1899), which was later subsumed into the taxon *Homo erectus* (Mayr, 1944, 1950), with the Trinil skullcap as its type fossil (Meikle and Parker, 1994). According to Dubois, all *Pithecanthropus* finds, including the four femora that were discovered decades after their excavation at Trinil (Dubois, 1932, 1934), derived from the same fossil-bearing layer, which he initially referred to as the 'Lapillischicht' (lapilli layer; Dubois, 1895, 1896, 1932, 1934), and later termed the 'Hauptknochenschicht' (main bone layer, hereafter referred to as H.K.; Dubois, 1908). However, immediately after Dubois' initial publications on *Pithecanthropus*, a fierce debate ensued that focused on the apparent taxonomic discrepancy between the archaic skullcap and the very modern-looking femur (e.g., Manouvrier, 1895; Hepburn, 1896).

Although Dubois' primary interest lay with the hominin fossils, he eventually published preliminary reports on the faunal assemblages from Trinil and other localities in the Kendeng area (e.g., Kedung Brubus), which he collectively defined as the Kendeng or Trinil fauna (Dubois, 1907, 1908). His collections and studies played a key role in the development of a biostratigraphic framework for Java and, through comparison with other Javanese and Asian faunas, the first (relative) age estimates for Trinil.

A second field campaign took place at Trinil between 1907 and 1908 under the supervision of Lenore Selenka. It consisted of an extensive excavation on the right bank (Grube I), and a smaller excavation on the left bank (Grube II), continuing where Dubois' 1907 excavations ended (see Fig. 2B). Although the campaign again yielded large quantities of vertebrate fossils, no additional hominin remains were found (Selenka and Blanckenhorn, 1911). During the campaign, more attention was paid to the geology of the Trinil site and the wider area, notably by the geologists Dozy and Carthaus. The flora and fauna from Trinil were described in detail in 1911 by a

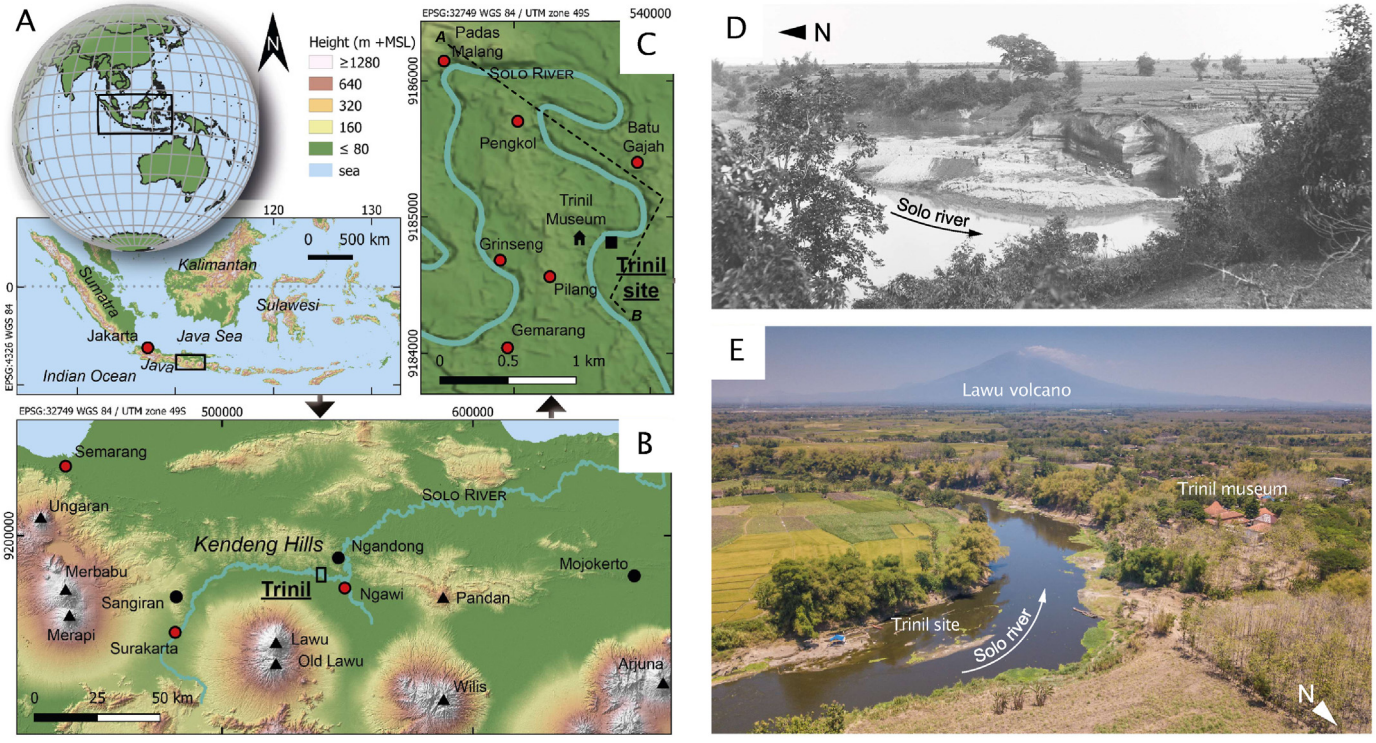

Fig. 1. A) Global location and topographical map of the Indonesian archipelago. B) Topographical map of central/east Java showing the location of Trinil as well as the locations of other key fossil-bearing sites (black dots), major cities (red dots), and volcanoes (triangles). C) Local map of Trinil and surroundings with the Trinil site (black filled square), the Trinil Museum, and nearby villages (red dots). D) Overview of the Dubois excavation mid-November 1900 (Historic photo collection number DUBO1494). E) Aerial photograph looking to the southwest and showing the site, museum, and the Lawu Volcano in the background.

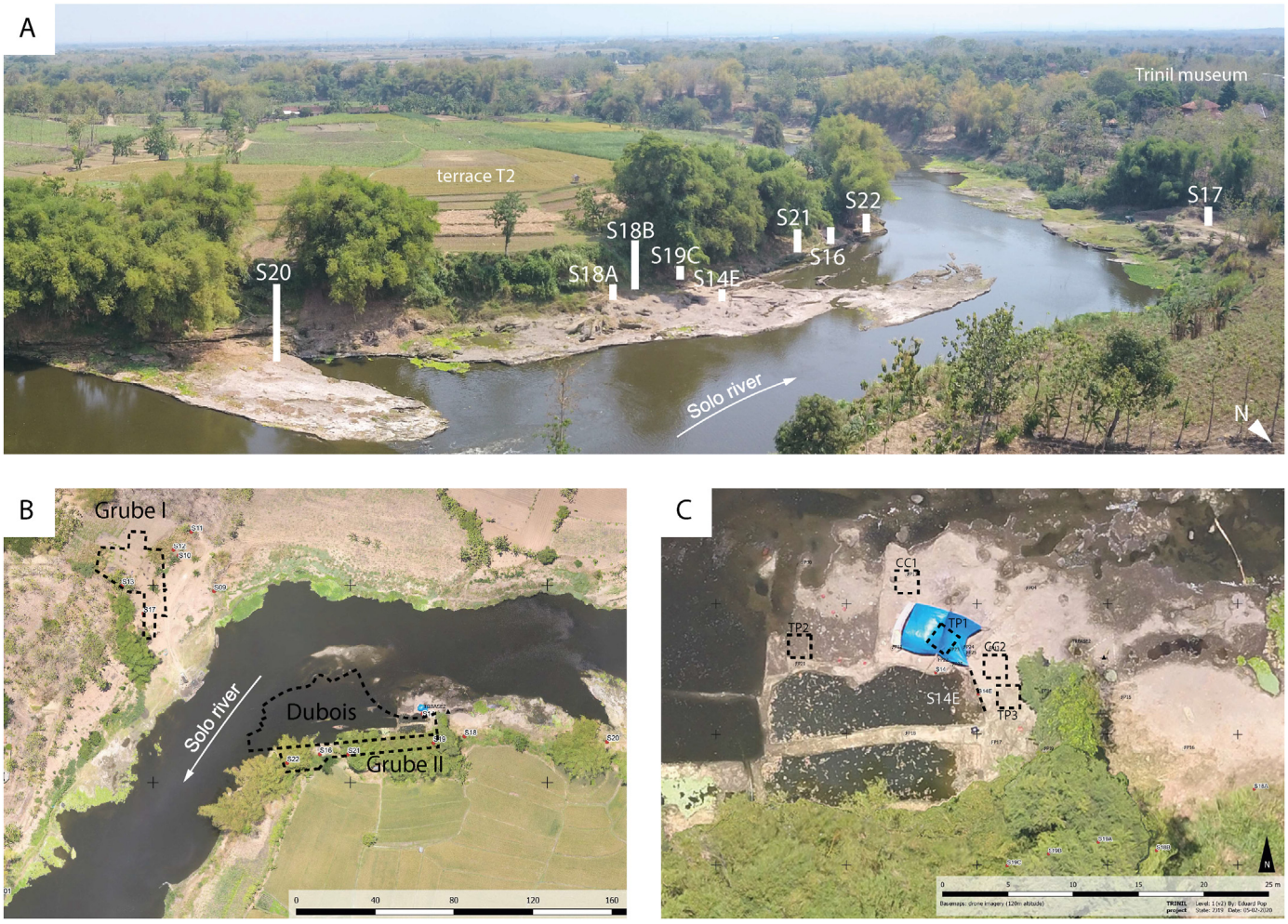

Fig. 2. A) Aerial photograph from the right Solo River bank looking south towards the Trinil site with the location of the stratigraphic sections. B) Vertical, orthorectified aerial photograph showing the location of the documented sections as well as the approximate location and outline of the Dubois (1891–1900) and Selenka (1907–1908; Grube I–III) excavation pits. Black lines in Grube I indicate the locations of stratigraphic profiles A and B (Dozy, 1911) and 2 (Carthaus, 1911). C) Vertical, orthorectified aerial photograph of the eastern end of the historical excavation area where there are still outcrops of the highly fossiliferous deposits remaining north of the river bank. Indicated are the locations of the test pits (TP1, TP2, and TP3), and clast count localities (CC1 and CC2).

multidisciplinary team of specialists including Stremme, Martin-Icke, and Schuster (see Selenka and Blanckenhorn, 1911) whose age assessments—in most cases based on the proportion of extinct and extant fauna—varied from late Pliocene to early Pleistocene (Blanckenhorn, 1911).

A large body of research was conducted over the course of the 20th century—including additional fieldwork at Trinil, as well as chemical analyses on fossils, radioisotopic dating, and comparative faunal studies with other key sites on Java. A comprehensive overview of the research history of the Trinil site is provided in SOM Text 1. Despite this extensive research, many critical issues surrounding the Trinil site have not yet been resolved. For example, the position of Femur I in the hominin evolutionary framework of SE Asia has been discussed as recently as 2015 (Ruff et al., 2015). Also, the recently obtained age range of 640–380 ka for sediment infills of fossil bivalve shells from Trinil assumed to originate from the H.K. (Joordens et al., 2015), has not been reconciled with the substantially older age estimate of ~0.9 Ma for a Trinil H.K.-like fauna recovered from the Grenzbank at Sangiran (de Vos et al., 1982; Leinders et al., 1985). While the geochronology of the hominin-bearing deposits at Sangiran and Ngangdong (Fig. 1B) has been refined (Matsu'ura et al., 2020; Rizal et al., 2020), the age of Trinil remains uncertain. The key role that it plays in paleoanthropology and the biostratigraphy of insular SE Asia warrants a fresh look at the chronostratigraphy of the Trinil site, based on new fieldwork and a comprehensive dating study.

Fieldwork was carried out at and around Trinil to obtain a better understanding of the geology of the wider Trinil area, and the (chrono)stratigraphy of the Trinil site. The present paper aims to provide a detailed (chrono)stratigraphic framework for Trinil that allows us to address the age controversy of Trinil and its fossil fauna, including the hominin fossils. To that end, the stratigraphy of the left-bank Trinil site was documented in detail by logging stratigraphic sections and smaller-scale test pits dug in the river-bank, covering the limited remnants of the highly fossiliferous deposits targeted by the historical excavations. To obtain age control for the identified units, specifically the highly fossiliferous ones, we applied a combination of $^{40}Ar/^{39}Ar$, feldspar post-infrared stimulated luminescence ($pIRIR_{290}$), and magnetostratigraphic dating methods. We discuss the implications of this chronostratigraphic study, focusing on the debated contemporaneity of the Trinil faunal assemblage (including the hominin remains), the degree of reworking of sediments and fossils, and the role of the Trinil fossils in the biostratigraphy of Java.

1.1. Geological background of the Trinil site

Berghuis et al. (2021) developed a stratigraphic framework for the greater Trinil area, revising the system devised by Duyfjes (1936), and reconstructed the local landscape changes over time including the development of Solo River terraces. The pre-terrace stratigraphy of the Trinil area comprises the Late Pliocene marine Kalibeng Formation, followed by the Early Pleistocene lagoonal Padas Malang Formation. After emerging, the plains around Trinil consisted of coastal marshes that were frequently overrun by volcanic andesitic lahars which were occasionally incised and reworked by rivers. These terrestrial deposits constitute the Batu Gajah Formation. The overlying late Middle Pleistocene Trinil Formation reflects a change in the volcanic regime from andesitic towards more explosive dacitic volcanism. This volcanism resulted in the formation of a barrier that isolated the plains of the Trinil area from the marine base level in the south, thereby creating the Ngawi paleolake basin. The pre-terrace formations dip ca. 2–10° to the south and crop out along the Solo River in the present day (Berghuis et al., 2021).

These pre-terrace deposits are incised and overlain by the terrace deposits of the Solo Formation, which consists of at least seven terraces (T7–T1, Fig. 3; Berghuis et al., 2021). Berghuis et al. (2021) tentatively correlate these terraces around Trinil with the similarly spaced terraces in the Kendeng Hills of which the oldest yielded luminescence ages of 358 ± 26 and 316 ± 36 ka and the youngest was dated at 31 ± 6 ka (Rizal et al., 2020). Berghuis et al. (2021) inferred that the outcrops of the Batu Gajah Formation at the eastern end of the Trinil historical excavation site are directly overlain by T2 terrace deposits, which have been dated to 95^{+56}_{-36} ka at nearby Grinseng, and tentatively correlated to the Ngangdong terrace in the Kendeng Hills area (Berghuis et al., 2021) dated to 140–92 ka (Rizal et al., 2020).

2. Materials and methods

2.1. Stratigraphy

Geological fieldwork was carried out at and around the Trinil site in 2016, 2018, and 2019 at the end of the dry season (September–October) when the river water level was at its lowest. This allowed us to log and sample as much of the stratigraphy as possible in the present-day riverbank and in the deposits near the low water level where the historical excavations took place (Fig. 2).

Sections Seven ca. 1–2 m wide sections (S18A, S18B, S19C, S14E, S21, S16, and S22) were dug and cleaned at the left river bank of the Trinil site (Fig. 2A and B). The location of these sections was chosen based on accessibility and even distribution along the entire ca. 90 m length of the old east-west back wall of the Dubois excavation and Selenka Grube II excavation (Fig. 2B). In addition, at the left bank eastward of the Trinil site, S20 was documented to aid in linking these sections to the larger-scale schematic stratigraphic cross-sections of Berghuis et al. (2021). Although this paper focuses on the left bank, a ca. 3 m wide section (S17) on the right riverbank was also studied and sampled for $pIRIR_{290}$ dating.

To document the exact spatial position (including elevation) of the stratigraphic sections, a dGPS system (GPS Sokkia GRX-2) with a base station and rover was used to measure multiple reference points within the sections. Ellipsoidal heights (WGS84) were converted to orthometric height (meters above sea level; m + MSL) by subtracting the local geoid height (EGM96) of 25.142 m. The sections were subsequently logged and photographed with dGPS-measured reference markers in place. Sets of images of each section were processed by Agisoft Metashape Professional v. 1.4.5 (Agisoft LLC, St. Petersburg) into 3D models and vertical orthophotos. After documentation, the sections were sampled for sedimentological and geochronological analyses.

Test pits Three test pits with a surface area of ca. 1 m^2 were dug directly into the remains of highly fossiliferous outcrops at the eastern part of the Trinil site (TP1, TP2, and TP3; Fig. 2C). These test pits provide a detailed insight into the stratigraphy where it was not possible to construct larger sections. They also provide insight into the vertical fossil distribution within the exposed deposits, facilitating the identification of the primary target layer(s) of the historical excavations. Furthermore, the test pits yielded a reference assemblage of fossils with a carefully documented provenance for future zoological, taphonomic and direct dating studies. Exposed finds were measured with dGPS, removed, labeled, documented, and stored in the Trinil Museum. All sediments excavated from the test pits were wet-sieved on sieves with mesh sizes of 5 and 2 mm to recover fossil faunal and plant macro remains. Sieving also yielded hornblende crystals used for $^{40}Ar/^{39}Ar$ dating.

Clast count To assess the clast composition of the fossil-rich layers at the Trinil site, a gravel composition count was done at CC1 and CC2 (Fig. 2C), targeting respectively the lower and upper

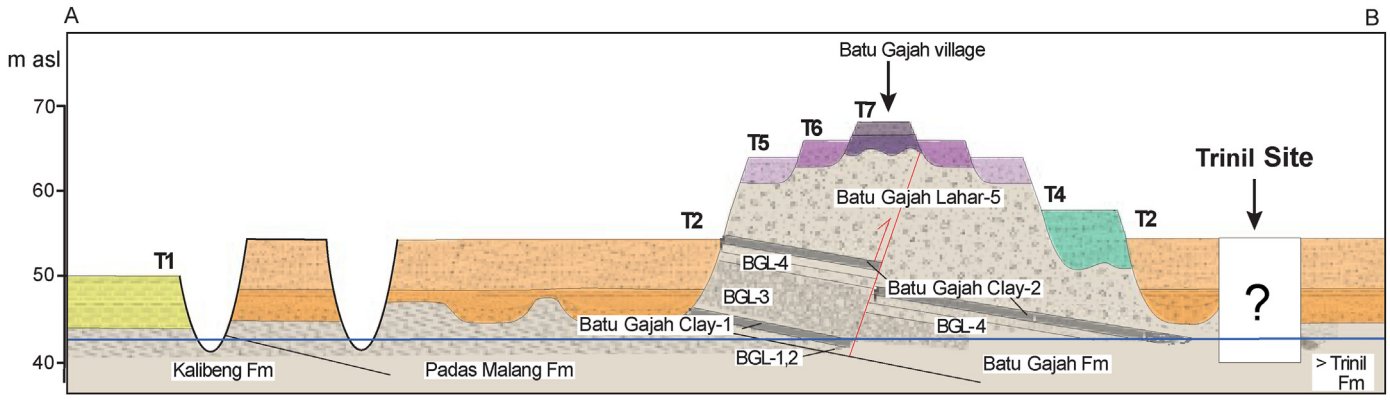

Fig. 3. Schematic and idealized cartoon of the recently revised, large-scale stratigraphy of the regional Trinil area (adapted from Berghuis et al., 2021; see Fig. 1C for the location of cross-section A-B). At the base lies the south-dipping pre-terrace stratigraphy comprising the Late Pliocene Kalibeng, Early Pleistocene Padas Malang, Pleistocene Batu Gajah, and Middle Pleistocene Trinil Formations. The horizontal terrace stratigraphy of the Solo Formation is situated on top of and cutting into the pre-terrace stratigraphy, and is subdivided into at least seven terraces (T7–T1, from old to young). The approximate location of the Trinil site is indicated. BGL=Batu Gajah Lahar. The horizontal blue line indicates Solo river water levels during field work.

fossiliferous layer as identified in the test pits. A minimum of 100 clasts >15 mm was collected from a surface area of 1 m^2, separated into lithological categories, and counted. Bioclasts, including fossils, were omitted from the count.

2.2. Geochronology

$^{40}Ar/^{39}Ar$ dating A total of 18 samples for $^{40}Ar/^{39}Ar$ dating were taken from detrital sediments that lacked clear evidence of recent bioturbation as well as from individual andesite and pumice clasts (see Fig. 4 for locations). The samples were processed and analyzed at the Vrije Universiteit (VU, Amsterdam, NL; see SOM Text 2 for details). Ages were calculated with decay constants of Min et al. (2000) and using an age of 28.201 Ma for the Fish Canyon Tuff standards (Kuiper et al., 2008). The final depositional age depends on the measurement protocol and is based on inverse isochron analyses or statistical interpretation of the measured age distribution. All final age calculations are presented at the 2σ level. Based on the detrital context all samples are considered to have been reworked, and as such they only provide a maximum depositional age.

Paleomagnetism A total of 92 paleomagnetic samples were collected during the fieldwork campaigns of 2018 and 2019. Approximately 2.5 cm long cores were taken from cleaned, freshly exposed sediments using a battery-powered hand drill (see Fig. 4 for sample locations). Samples were oriented using a Pomeroy orientation device with a Brunton compass. Where possible, at least two or three samples per level were drilled to compensate for broken cores and to allow application of both thermal (TH) and alternating field (AF) demagnetization methods. For logistical reasons, the demagnetization and measurement of the 2018 and 2019 sample sets were performed at two different paleomagnetic laboratories, the Paleomagnetic Laboratory Fort Hoofddijk (Utrecht, NL) and the GeoForschungsZentrum (GFZ Potsdam, Germany), respectively. The Characteristic Remanent Magnetization (ChRM) directions were determined on orthogonal vector projection diagrams of demagnetization paths using Paleomagnetism.org (Koymans et al., 2016). ChRM's were divided into four classes: class 1 with a reliable direction and reliable polarity, class 2 with an unreliable direction and reliable polarity, and class 3 with an unreliable direction and unreliable polarity. A fourth class includes samples which broke during transport, had unclear markings, or yielded no interpretable directions. For the interpretation of the Trinil magnetostratigraphic record, only class 1 and 2 samples were considered for the determination of the paleomagnetic polarity.

To further assess the various magnetic minerals present in the samples and their behavior upon thermal treatment, six representative paleomagnetic samples were processed on a modified Curie balance at the Paleomagnetic Laboratory Fort Hoofddijk (Utrecht University, The Netherlands). For further details on the magnetostratigraphy and Curie balance measurements see SOM Text 3.

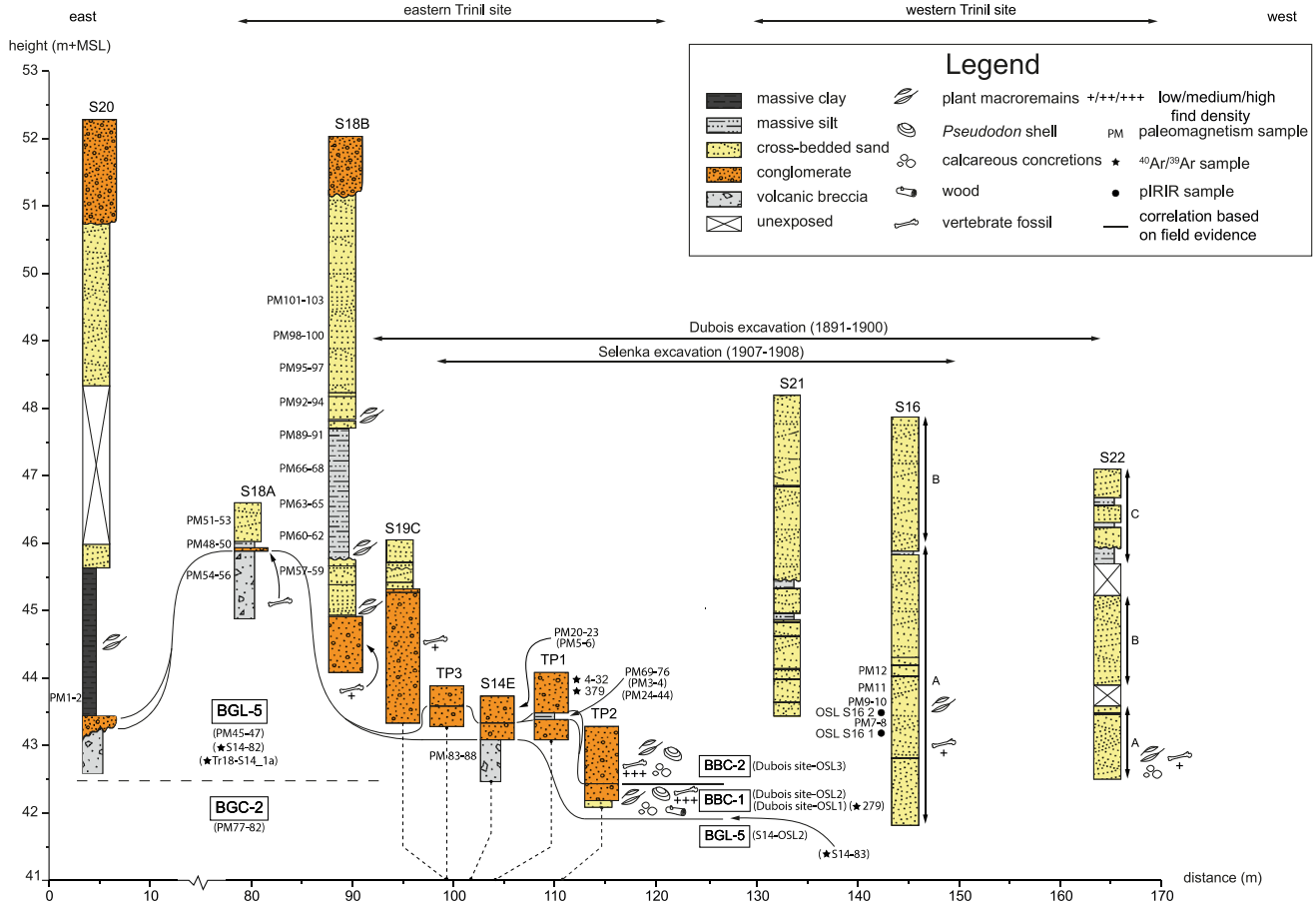

Fig. 4. Overview of the Trinil site lithostratigraphy, including the documented sections and testpits. Further indicated are the sampling locations of the $^{40}Ar/^{39}Ar$, $pIRIR_{290}$, and paleomagnetic samples, and the extent of the historical excavations relative to the documented sections. BGC-2 = Batu Gajah Clay 2, BGL-5 = Batu Gajah Lahar 5, BBC-1 = Bone Bearing Channel 1, BBC-2 = Bone Bearing Channel-2, T2 = Terrace 2. Samples from outcrops are given in parentheses.

Feldspar infrared luminescence dating Seven luminescence samples were taken from freshly exposed sediments in well-documented and georeferenced sections, or from cleaned, pre-existing outcrops of known stratigraphic position (see Fig. 4 and SOM Fig. S1H for sampling locations). For a more detailed description of the luminescence approach see SOM Table S1 and SOM Text 4. Samples were taken by hammering a 7 cm diameter stainless steel tube into the sediment or, if the sediment was too consolidated, carving out a block of ca. 25 × 25 × 25 cm. After sampling, samples were wrapped in aluminum foil and covered in duct tape to prevent exposure to daylight and avoid the mixing of sediments within the tubes and blocks. The samples were processed at the Netherlands Centre for Luminescence dating (Wageningen University, NL). Each sample was subsampled for dose rate (D_r) and equivalent dose (D_e) measurements. For D_e measurements the coarse-grained K-rich feldspar was separated. Luminescence equivalent doses were determined based on the post-IR IRSL (stimulation temperature 290 °C) single-aliquot protocol (termed $pIRIR_{290}$, Buylaert et al., 2012). The dose response curves were mathematically constrained using single saturating exponential fits and final palaeodoses were calculated based on the average of the accepted single aliquot D_e values. For D_r determination, the activity concentrations of the U and Th decay chains and ^{40}K were measured using high-resolution gamma-ray spectrometry. The concentrations were converted to dose rates using the conversion factors of Guérin et al. (2011)) and the soft matter attenuation based on Madsen et al. (2005). The contribution of the cosmic dose rate was calculated based on Prescott and Hutton (1994). The final luminescence age was calculated by dividing the $pIRIR_{290}$ palaeodose by the dose rate.

3. Results

3.1. Stratigraphy

The stratigraphy of the Trinil site as exposed in the 2018 and 2019 sections, test pits, and outcrops is shown in Figs. 4–6. First, the stratigraphy of the eastern part of the site will be described, where outcrops facilitate a straightforward correlation of the lower strata between sections, test pits, and clast count localities. Correlations between the three documented sections at the western part of the Trinil site and the stratigraphy of the eastern part of the site are less straightforward and are therefore presented separately. Detailed information is provided in the supplementary information including section drawings, orthophotos, and descriptions (SOM Figs. S1A–H and S3; SOM Text S2) and the results of the clast counts (SOM Table S2).

Eastern part of the Trinil site At the base of the eastern Trinil site on the left bank of the Solo River lies a dark grey, massive clay, Batu Gajah Clay 2 (BGC-2; sensu Berghuis et al., 2021) that is only visible in outcrops at low water levels (ca. 42.5 m + MSL; Fig. 5A). Where exposed, the top of the clay appears to be more or less horizontal. From this outcrop, a single, well-preserved vertebrate fossil was recovered.

Overlying the clay and extensively exposed in outcrops and sections (S20, S18A, S14E) is a poorly-sorted, matrix-supported volcanic breccia, Batu Gajah Lahar 5 (BGL-5; sensu Berghuis et al., 2021). The volcanic silty-sandy breccia contains clay clasts, weathered and unweathered volcanic fragments, and gravel-sized pumice. Occasionally, plant remains are found in the form of tree trunks. Vertebrate fossils are rare. The thickness of this layer—assuming a more or less horizontal contact with the underlying BGC-2—varies greatly, from only ca. 0.5 m at S20 to ca. 3 m at S18A and again ca. 0.5 m at S14E (Fig. 4). The breccia is dark grey and contains light grey-colored intrusions from the top (see SOM Fig. S1G). One of these intrusions is composed of sand-sized volcanic glass fragments. Reconstructing the exact processes resulting in these highly complex structures is beyond the scope of this paper, but internal lahar dynamics and/or fault-related tectonic activity are likely possibilities.

Ca. 10 m to the west of S18B, the BGL-5 is overlain by a poorly-sorted silty-sandy conglomerate, as visible in outcrops (Fig. 5A–C), in S14E (SOM Fig. S1G), and TP1-3 (SOM Fig. S3). The unconformable contact with the BGL-5 and the lithology of the conglomerate indicates that the BGL-5 was fluvially incised. Clasts within this conglomerate consist predominantly of volcanic rocks (76%) in various levels of rounding and weathering, and carbonate concretions (23%; SOM Table S2). The conglomerate is characterized by the occurrence of silty lenses, especially in outcrops just east of the Trinil site. Furthermore, it is rich in freshwater aquatic invertebrates, notably shells of the bivalve mollusk *Pseudodon vondembuschianus trinilensis*, and aquatic as well as terrestrial vertebrate fossils, notably a *Stegodon trigonocephalus* tusk in TP3 (Fig. 5D). The fossils are characterized by heterogenous fossilization conditions. No vertebrate fossils were found in anatomical connection and a high percentage is fragmented. In contrast, many *Pseudodon* shells are intact and the valves articulated. The deposit also contains plant macro remains (e.g., wood, including logs in surface exposures and branches in TP2; see SOM Fig. S4A). This fossil-rich deposit, which is interpreted as an erosion-generated skeletal channel lag assemblage (sensu Rogers and Kidwell, 2007), is assigned the name Bone-Bearing Channel 1 (BBC-1). In some locations at the Trinil site, the top of the BBC-1 consists of a thin (~10–20 cm) silt layer or lens (visible in surface outcrops as well as in TP1; see Fig. 5B and C), which yielded occasional *Pseudodon* shells as well. Based on the dating evidence (see below) it is interpreted as a silty facies of the BBC-1 and is from now on referred to as the BBC-1 (s).

The BBC-1 is unconformably overlain by a planar cross-bedded, poorly sorted, fine conglomerate with a silty sand matrix which reaches a maximum observable thickness of 2–3 m and contains occasional well-sorted sand lenses. The clast composition in this fluvial conglomerate is comparable to that of the BBC-1 with predominantly (weathered) volcanic rocks (56%) but it contains almost twice as much carbonate concretions (40.5% vs 23.5%; SOM Table S2). The fossil find density of this layer is variable, ranging from low in the river bank sections S19C and S18B, to very high in S14E and TP1-3. This unit contains fossils of both aquatic (freshwater sharks, turtles, gharial, and crocodile) and terrestrial vertebrates, as well as plant remains. Shells of *Pseudodon vondembuschianus trinilensis* are relatively abundant. Notable terrestrial fossils include a *Stegodon trigonocephalus* mandible (findnumber 718) and a proboscidean tusk (findnumber 461; both in TP1). The fossils are characterized by heterogenous surface taphonomy which might indicate varying fossilization conditions. No fossils are found in anatomical connection and again a high percentage of fossils are fragments (~72.5%). This fossiliferous conglomerate is also interpreted to be a channel lag deposit and is assigned the name Bone-Bearing Channel-2 (BBC-2). It is visible in sections S18B, S19C, S14E, and at the top of TP1-3. At S18A, a ca. 5 cm thick very fine gravel unconformably overlies the BGL-5 (SOM Fig. S1A). In this layer, which most likely correlates with the BBC-2, one vertebrate fossil has been found.

East of the Trinil site, at section S20 and notably on the flat outcrop extending far into the river (Fig. 2A), the BGC-2 and the overlying breccia BGL-5 are covered by a layer of poorly-sorted, clast-supported conglomerate consisting of well-rounded volcaniclastic gravel (SOM Fig. S3C). The conglomerate in S20 contains predominantly unweathered volcanic material, while weathered volcanic material and carbonate concretions—that dominate the

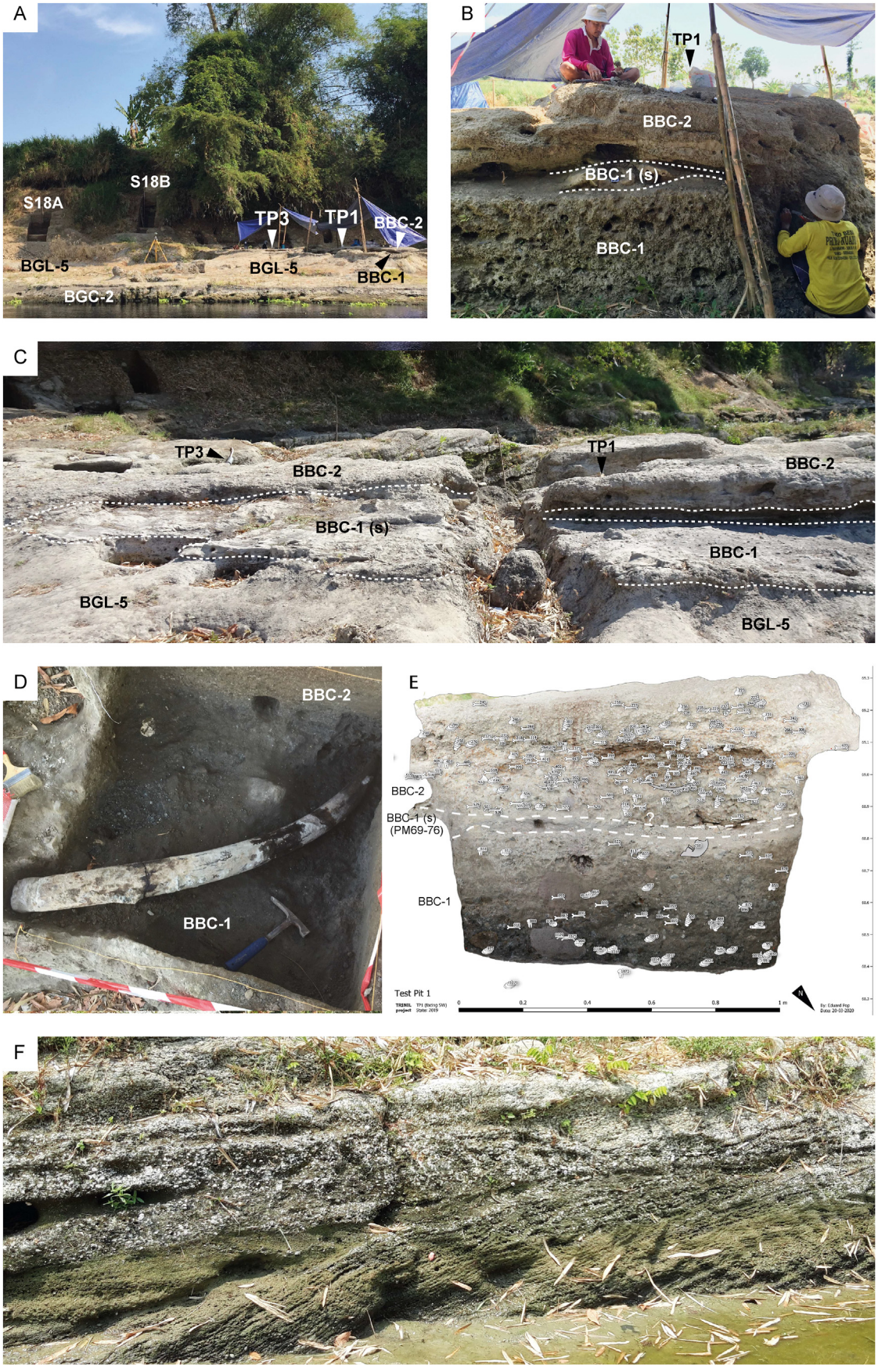
A
S18B
S18A
TP3
TP1
BBC-2
BGL-5
BGL-5
BBC-1
BGC-2
B
TP1
BBC-2
BBC-1 (s)
BBC-1
C
TP3
BBC-2
TP1
BBC-2
BBC-1 (s)
BBC-1
BGL-5
BGL-5
D
BBC-2
BBC-1
E
BBC-2
BBC-1 (s)
(PM69-76)
BBC-1
Test Pit 1
F

highly fossiliferous BBC-1 and BBC-2 (see above)—are rare. The conglomerate is poor in fossils. It is overlain by ca. 2 m of laminated, dark-colored clay consisting of millimeter to centimeter-thick layers that contains numerous plant macro remains. The conglomerate and the laminated clay have been interpreted as a channel lag and oxbow lake of the T2 terrace, respectively (Berghuis et al., 2021). As they are outside of the main Trinil site and lack fossils, these deposits will not be further considered here.

The deposits overlying the BBC-2 at the Trinil site are only exposed in the riverbank sections (S20, S18A, S18B, S19C; Fig. 4; SOM Fig. S2A-C, H). Apart from the gravels at > 51 m + MSL in S20 and S18B, these deposits are relatively fine-grained: cross-laminated/cross-bedded sands and silts and massive silty clay/clayey silts. Near the historical excavation area (S18B/S19C) the BBC-2 is overlain by ca. 1 m of cross-bedded sands and silts, of which the top 10–20 cm is cemented. A ca. 2 m thick, massive silty clay unconformably overlies it in S18B. This silty clay is rich in plant macro remains but did not yield any fossils. On top of the silt lies ca. 3.2 m of cross-bedded tuffaceous sands, silty sands, and sandy silts and ca. 80 cm of clast-supported gravel with rounded pebbles up to 5 cm in diameter, which both only rarely yield fossils. Above this lies the present-day soil level at ca. 53 m + MSL.

Western part of the Trinil site At the western part of the Trinil site lie sections S21, S16, and S22 (Fig. 4; SOM Figs. S2D–F). Although they all consist of cross-laminated/cross-bedded sands and silts with occasionally massive clayey silts and silty clays, it was not possible to make direct correlations between the sections. Based on explorative Edelman coring at S16, it was found that the sands and silts continue until at least 1.5 m below low-water level. The sediments in these western sections are comparable to those overlying the BBC-2 at S18B and S19C. Occasionally thin gravel layers are found in the larger cross-bedded structures, but units of similar texture, structure, and clast composition as the BBC-1 or BBC-2 are absent—also at equivalent heights at which these highly-fossiliferous conglomeratic units are documented in the east. Fossils are generally sparse in all three sections; a notable exception being two well-preserved, articulated, bovid vertebrae found in the lower part of S16 (Fig. 6A and B). Plant remains are occasionally found as well. *Pseudodon* shells are rare, only one valve fragment was found in S16. At the right bank of the river, S17 (NW from S22; Fig. 2A and B) revealed similar fluvial cross-laminated/cross-bedded sands and silts as in S21, S16 and S22 (SOM Fig. 1H).

3.2. Geochronology

^{40}Ar/^{39}Ar dating A summary of the ^{40}Ar/^{39}Ar data is presented in Table 1 and the full dataset in provided in SOM Table S3.

The first batch of ^{40}Ar/^{39}Ar measurements (VU110) was done on andesite hornblende from the BGL-5 (S14-82; VU110-T3), detrital hornblende from the interface between the BGL-5 and the BBC-1 (s) below the BBC-2 (S14-83; VU110-T4). All single grain measurements on these samples have large analytical uncertainties. Multigrain measurements (three and six grains per fusion) on the same samples have lower uncertainties, revealing age distributions spanning more than 1 Myr (SOM Table S3). The andesite clast from the BGL-5 yielded an inverse isochron age of 0.71 ± 0.12 Ma (2σ, VU110-T3; SOM Fig. S5). The inverse ^{40}Ar/^{36}Ar isochron intercept of 399.7 ± 8.2 suggests the presence of extraneous Ar. For sample VU110-T4 we were unable to define a reliable depositional age.

The second batch (VU116) consists of large phenocrysts from the BBC-2 (n = 13; VU116-T1 to VU116-T12 and VU116-T16), detrital hornblende from BBC-1 and BBC-2 sediment samples (n = 2; VU116-T13 and VU116-T14), and one pumice clast from the BBC-1 (VU116-T15) on which both single grain and multigrain measurements were successfully carried out. One of the large phenocrysts from the BBC-2 (VU116-T16) gave very low ^{40}Ar* yields compared to the other phenocrysts and was rejected. For the other phenocrysts (VU116-T1-T12), a large spread in ages both within and between hornblende crystals was observed (SOM Fig. S6), indicating a complex magmatic history with different growth periods. Alternatively, argon loss in some parts of the crystal may explain the younger ages. The resulting ages of the large hornblende crystals were deemed unusable to determine a reliable maximum depositional age.

For the two sediment samples of batch VU116, we dated, in addition to multigrain experiments, numerous single grain hornblende crystals ($n \approx 100$) with the assumption that the youngest age population approaches the depositional age. For sample VU116-T13 from the BBC-1, 94 out of 96 total fusion, single grain measurements on detrital hornblende were successful and yielded reliable ages ranging from 0.75 ± 0.28 to 4.05 ± 0.55 Ma (2σ, Fig. 7A). A single measurement of 70 ka (i.e., the youngest) was rejected due to the low ^{40}Ar* content (0.11%). The resulting three measurements have a weighted mean age of 0.77 ± 0.12 Ma (2σ) which is interpreted as the maximum depositional age for the BBC-1.

For sample VU116-T14 from the BBC-2, 92 out of 93 single grain measurements were successful, yielding reliable ages ranging from 0.35 ± 0.75 to 2.68 ± 0.26 Ma (2σ, Fig. 7B). Using a similar approach as for VU116-T13, the youngest age group of VU116-T14 (n = 11) yielded a weighted mean age of 0.45 ± 0.11 Ma (2σ), which is interpreted as the maximum depositional age for the BBC-2 and which likely lies close to its actual depositional age.

A tentative age for the pumice clast from the BBC-1 (VU116-T15) was calculated at 0.96 ± 0.04 Ma (2σ; Table 1) by ordering the measurements from young to old and starting from the youngest age, adding measurements until the critical mean square of weighted deviates threshold was crossed (method as described in Schaen et al., 2020).

Paleomagnetism The paleomagnetic samples come from 16 sampling locations, 7 stratigraphic sections, and 11 isolated outcrops covering most of the identified stratigraphic units with a large range of lithologies (Fig. 8; SOM Table S4; SOM Fig. 7). Samples generally have a strong initial natural remanent magnetization intensity which is probably related to their volcaniclastic origin. Almost all samples from Trinil are characterized by a strong low coercivity/temperature component (LCC/LTC) up to 20–30 mT/200–250 °C and high viscosity. After removal of this LCC/LTC component, most samples display a high temperature/high coercivity (HTC/HCC) component from 30 to 50–100 mT/200 to 350–450°C. In only a few samples, either erratic directions or full demagnetization at low levels resulted in demagnetization paths from which no reliable results could be obtained (Class 4). Clay samples from the BGC-2 and BGL-5 deteriorated during thermal treatment and yielded uninterpretable AF demagnetizations such that no directions could be determined from these layers. In the rest of the samples, almost all demagnetizations are characterized by two components (Fig. 8). Most of the LCC/LTC indicate a normal

Fig. 5. A) View (looking south) on the eastern part of the Trinil site, showing the BGC-2, BGL-5, BBC-1, and BBC-2, and the location of various sections and testpits. B) View towards the north from a historical excavation pit south of TP1 (see Fig. 3C) showing the BBC-1 silt (s) situated between the BBC-1 and the BBC-2 (Catur Gumono is sitting on top of the BBC-2). C) overview of the typical BGL-5, BBC-1, silt, and BBC-2 succession as seen from the same direction as (A). D) Photo of TP3 showing an in situ fossil *Stegodon* tusk sticking out of the BBC-1 and up into the BBC-2. E) Orthophoto of TP1 showing BBC-1, BBC-1 (s), and BBC-2. F) Large scale east-west oriented bedding structures in the BBC-2 are visible in the excavation pits walls of an old excavation pit.

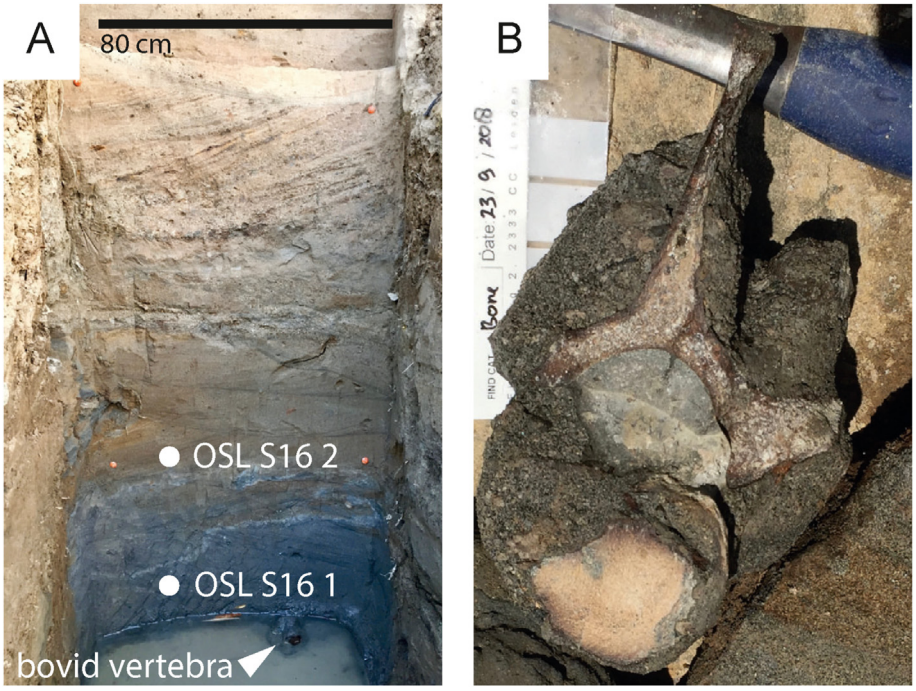

Fig. 6. A) Photo of the lower part of S16A (ca. 42.5 m + MSL–46 m + MSL, showing bluish-grey, cross-bedded sands from which luminescence dating samples S16-OSL1 and S16-OSL2 were taken (indicated). The white arrow points at the in situ fossil bovid vertebrae found in anatomical connection (shown in B) situated near the low water level of the Solo River. B) Photo of the same bovid vertebrae surrounded by sandy matrix immediately after its recovery. Note the brown color of the fossil, the complete spinous process, and the presence of a calcite infill in the vertebral foramen.

Table 1
Summary overview of $^{40}Ar/^{39}Ar$ ages.[a] obtained from sieving residue.[b] single grain measurements in this batch were unsuccessful.[c] number of analyses included in the age calculation versus total measurements.

								maximum depositional age				
VU ID	sample	section	stratigraphic layer	source	grainsize	n grains/ fusion	method	age	± 2σ (Ma)		MWSD	n
VU110-T3	S14-82	outcrop	BGL-5	andesite clast	125–500 μm	1[b],3,6	inverse isochron age	0.71	±	0.12	1.25	6/20
VU116-T13	279	outcrop	BBC-1	sediment[a]	250–500 μm	1,3	weighted mean age of youngest grains (see text)	0.77	±	0.12	0.02	4/96
VU116-T14	379	TP1	BBC-2	sediment[a]	250–500 μm	1,3	weighted mean age of youngest grains (see text)	0.45	±	0.11	0.17	11/93
VU116-T15	Tr18-S14_1a	outcrop	BBC-1	pumice clast	250–500 μm	1,3	youngest population with MSWD < *t*-test statistic	0.96	±	0.04	1.47	11/20

polarity direction suggesting they reflect a recent normal overprint. The observation of a HTC in expected reversed polarity orientations, suggest a primary origin for the associated magnetizations. In many samples the LCC/LTC strongly overlapped the HCC/HTC on a significant coercivity/temperature range, such that component separation was difficult and resulted in stronger apparent scatter in the obtained HCC/HTC directions. These samples were thus usually labeled as Class 2 (reliable polarity but unreliable direction). Yet this incomplete overprint removal and resulting scatter does not affect the reliability of the determination of the polarity, especially for reversed orientations that can be clearly distinguished from their normal overprints. These demagnetizations with dual polarities were used to define the extent of the LCC/LTC. Demagnetizations that were defined below that extent were assumed as potentially overprint and thus not considered to determine the primary paleomagnetic polarity. Demagnetizations with persistent HCC/HTC in normal polarity orientations were carefully interpreted as they may be difficult to distinguish from a recent secondary overprint in the normal direction and should generally be considered with caution compared to reversed directions.

Along with demagnetization behaviors, Curie balance thermomagnetic measurements enabled us to better assess the origin and reliability of the ChRM (SOM Fig. S8; SOM Table S5; SOM Text S6). The results mainly show reversible heating-cooling curves with most of the magnetization decrease around 500 °C, typical of magnetite. This, in view of the volcanic lithologies and the generally high intensities and low coercivities, suggests that magnetite of a volcanic origin holds a major component of the remanence. Generally, the rock magnetic behaviors support our interpretation of a secondary origin for the LCC/LTC from very low coercivity magnetite-like carriers, while the HCC/HTC more likely represent a primary magnetization from more stable magnetite-like carriers.

To interpret the magnetostratigraphy, all the paleomagnetic results were positioned according to their respective stratigraphic units. At the top of the sampled stratigraphy, the upper part of the sandy terrace sediments of the Solo Formation yielded relatively

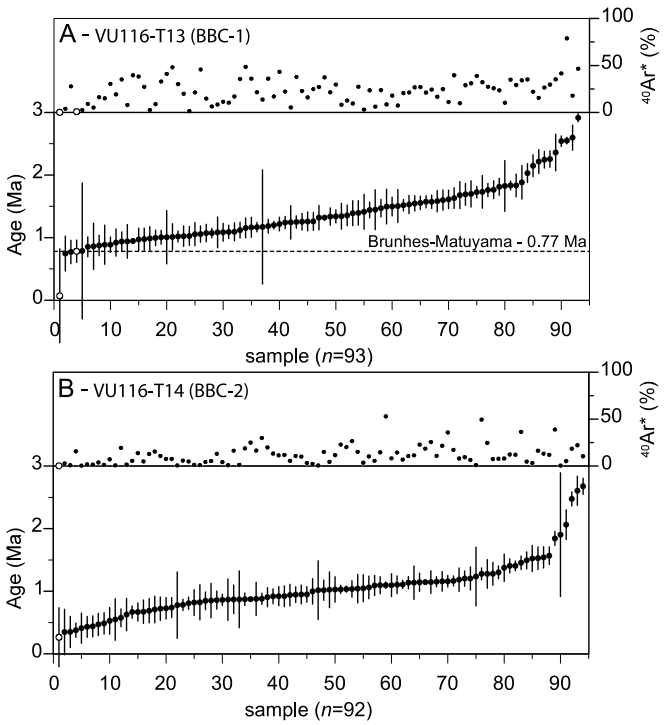

Fig. 7. Overview of all single grain, total fusion Ar/Ar data of detrital hornblende crystals from the BBC-1 and BBC-2 (analytical uncertainties are given in 1σ). A) Single grain measurements from a sample of the lower fossiliferous layer, BBC-1 (sample 279). B) Single grain measurements from a sample of the upper fossiliferous layer, BBC-2 (sample 379).

straightforward results with clear demagnetizations indicating mostly reliable normal polarities (class 1 and 2 directions; Fig. 8F). The lower, more silty part of the terrace had more unreliable directions (class 3) but sufficient reliable ones to indicate a normal polarity. The terrace sediments notably yielded two samples of reversed polarity (PM98 and PM90) that may relate to spurious overprints in seemingly reversed polarity orientation or to short paleomagnetic excursions. The BBC-2 has fewer samples ($n = 6$) and the demagnetizations are relatively noisy, which may be attributed to the coarser grain-size of this unit. Yet most samples ($n = 5$) yielded normal polarity orientations. The BBC-1 (s) has been more intensely sampled ($n = 43$) due to its silty lithology that is more promising for paleomagnetism, and to confirm preliminary 2018 results suggesting reversed polarities. Most samples ($n = 33$) yield a clear reversed polarity while remaining unreliable samples are concentrated in the TP1 section (Fig. 8E). In the BGL-5, mixed paleomagnetic results were obtained from only 10 samples collected at three locations. Reliable polarities (class 1 and 2 directions) are dominantly reversed, and the unit BGL-5 is therefore interpreted as reversed in polarity given the generally less reliable normal polarity directions that may represent unresolved strong overprints. In the BGC-2, the six samples collected at one location are mostly unreliable except for one reversed (PM77; Fig. 8C) and one possibly normal (PM82). Based on these few samples the unit polarity remains undetermined with a preference for a reversed polarity. In summary, the upper units of the terrace sediments and the BBC-2 are of normal polarity while the BBC-1 is of reversed polarity.

Feldspar infra-red stimulated luminescence dating For an overview of all $pIRIR_{290}$ feldspar luminescence measurements (n = 7) see Table 2. Performing $pIRIR_{290}$ measurements on Trinil sediment proved challenging; all samples were poor in K-rich feldspar and relatively few aliquots contained a strong $pIRIR_{290}$ luminescence signal (signal strengths were first tested before measurement of the corresponding regenerative dose response curves). Two samples, one from the BGL-5 (NCL-8119012) and one from the BBC-2 (NCL-8316193), did not yield a sufficient number of aliquots with a $pIRIR_{290}$ signal (test dose error >20%) that was strong enough for a robust D_e estimation and were therefore rejected. The three samples from S16 and S17 show a large scatter in the D_e distributions, presumably due to mixing of relative well-bleached (neglectable inherited age) and relative poorly bleached grains (significant inherited age), resulting in large palaeodose and thus age uncertainties. Unfortunately, these samples yielded too few aliquots with a suitable signal to better constrain the most robust D_e population and therefore the resulting ages have to be regarded as unreliable (see SOM Text 7). The two samples from the BBC-1 (s), NCL-8316192 and NCL-8316235, yielded more reliable results (Fig. 9). When applying an exponential fit approach to the two samples, the average natural $pIRIR_{290}$ signal at the 2D0 threshold (indicative of the onset of signal saturation) is reached for significant parts of the corresponding D_e distributions, resulting in minimum ages of >464 and > 422 ka, respectively.

4. Discussion

4.1. Trinil stratigraphy and age model

Based on the results above, a chronostratigraphic model can be constructed for the Trinil site (Fig. 10). First, the basal succession will be discussed, which can be correlated with the Batu Gajah Formation, and which is part of the pre-terrace stratigraphy, followed by the younger, overlying terrace deposits of the Solo Formation.

Pre-terrace stratigraphy At the base of the stratigraphy lies a black clay that is identified as the Batu Gajah Clay 2 (BGC-2; sensu Berghuis et al., 2021). It is only visible in outcrops at the eastern end of the Trinil site. No ages and reliable paleomagnetic results are available, but the BGC-2 must be older than the overlying volcanic breccia (BGL-5, sensu Berghuis et al., 2021), which has a maximum depositional age of 710 ± 120 ka (2σ).

The volcanic breccia BGL-5 was subsequently incised, which was followed by the deposition of the fossiliferous conglomerate of the BBC-1. Single grain $^{40}Ar/^{39}Ar$ measurements on detrital hornblende provide a maximum age of 770 ± 120 ka for the BBC-1. As the full spectrum of single grain $^{40}Ar/^{39}Ar$ measurements for BBC-1 and BBC-2 samples appear to show more or less continuous volcanic activity, we infer that the $^{40}Ar/^{39}Ar$ based maximum depositional ages probably lie close to the true depositional age. Based on the chronological constraints provided by the underlying BGL-5 and the reversed paleomagnetic signal of the BBC-1 (s) (see below), the BBC-1 has an age between 830–773, which suggests that it was potentially deposited soon after the BGL-5.

The silt layer BBC-1 (s), that locally forms the top of the BBC-1 and underlies the BBC-2, yielded two luminescence minimum ages of >464 and >422 ka. It also yielded a reversed paleomagnetic signal, while overlying deposits with a reliable polarity mostly yielded a normal signal. Based on the constraints provided by the $^{40}Ar/^{39}Ar$ ages of the BBC-1 and the underlying BGL-5, as well as those obtained by luminescence dating for the silt layer itself, the reversed polarity signal in the BBC-1 (s) can either belong to the Matuyama chron or one of the reversed polarity excursion events during the Brunhes chron (e.g., Osaka Bay at ~680 ka, La Palma at ~580 ka or the Big Lost at ~540 ka, see Channell et al., 2020). Although it is impossible to exclude the possibility that the reversed polarity is due to one of these short-lived events, the chance of actually recording such an event in the generally coarse-

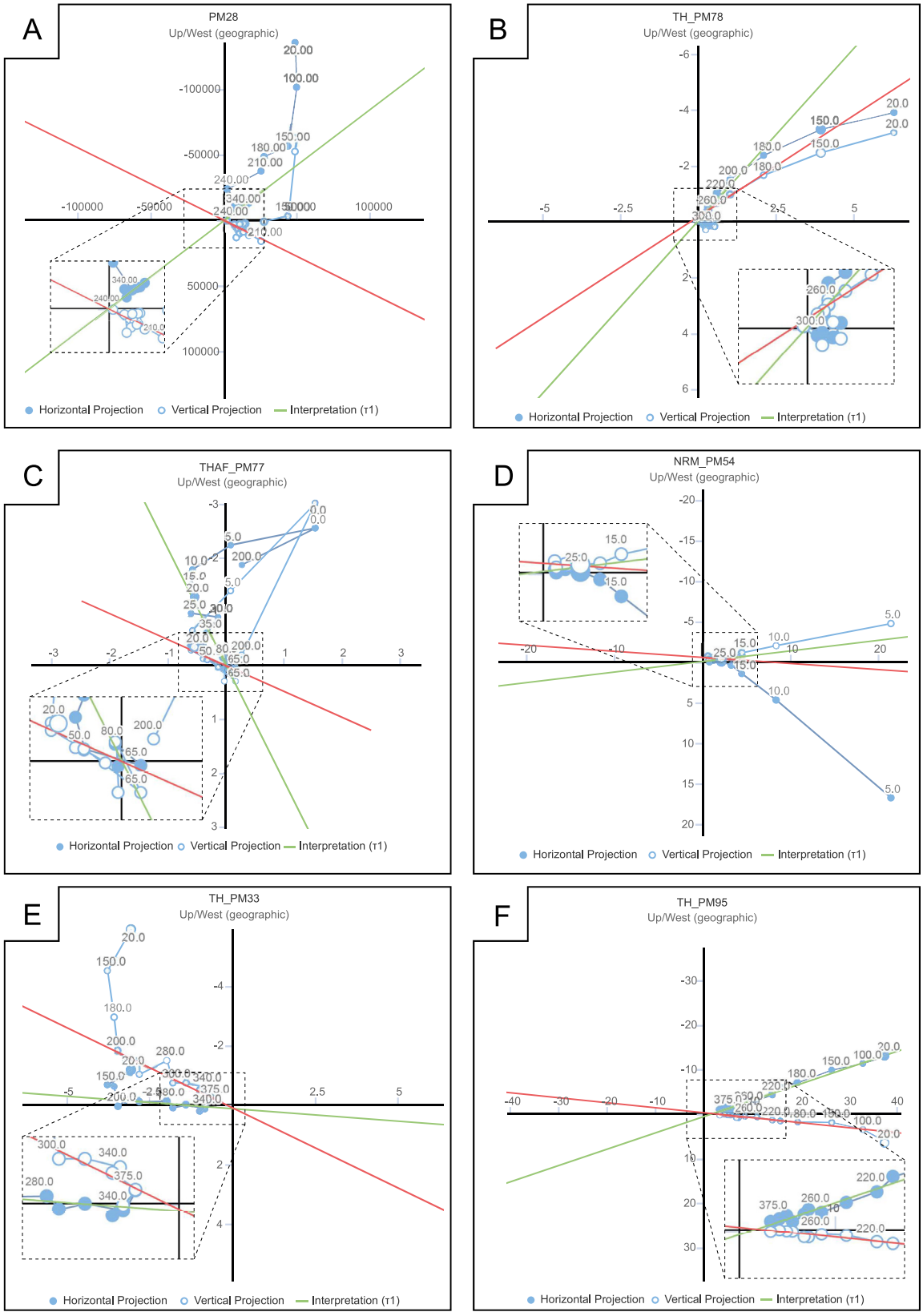

Fig. 8. A selection of vector endpoint diagrams of alternating field (AF) and (T) thermal demagnetized samples characteristic for Trinil. A) and B) class 3 samples, unreliable direction and an unreliable polarity, from BBC-1 (s) and BGC-2, respectively. C) and D) class 2 samples, unreliable direction and reliable polarity, from the BGC-2 and BGL-5, respectively. E) and F) class 1 samples, good direction and reliable polarity, BBC-1 (s) and T2 terrace, respectively. Coordinates are geographic up/West. See SOM Fig. S7 for a complete overview of all available vector endpoint diagrams and SOM Table S4 for their interpretation.

Table 2
Summary overview of feldspar pIRIR290 luminescence ages. Samples NCL-8316192 and NCL-8316235 are both in saturation and thus yield only minimum ages. Samples NCL-8119012 and NCL-8316193 failed. Samples NCL-8119013, NCL-8119017, and NCL-8119018 yielded finite ages.[a] number of accepted aliquots versus measured aliquots.[b] this apparent palaeodose represents the mean of the aliquots below saturation and needs to be taken with caution.[c] age is corrected for a pIRIR290 remnant dose of 30 ± 15 Gy (Joordens et al., 2015). For details see text.[d] significant part of the corrected age distribution plots above the saturation threshold (2D0). A minimum age is calculated based on the 2σ confidence interval, i.e. 95% confidence that the true age is larger than the minimum age.

NCL	Sample	Layer	n[a]	Palaeodose [Gy]	error −/+	Dose rate [Gy/ka]	error −/+	Luminescence age (ka)[c]	error −/+
8316235	TRI2016-Dubois site-OSL1	BBC-1 (s)	6/6	*586*[b]	*73*	1.17	0.07	**>422**[d]	**-**
8316192	TRI2016-Dubois site-OSL2	BBC-1 (s)	6/6	*833*[b]	*99*	1.31	0.08	**>464**[d]	–
8316193	TRI2016-Dubois site-OSL3	BBC-2	–	–	–	–	–	–	–
8119012	OSL S14 2	BGL-5	–	–	–	–	–	–	–
8119013	OSL S17 1	S17	12/12	109	21	1.41	0.09	**77**	**15**
8119017	OSL S16 1	S16	6/6	157	78	1.22	0.08	**129**	**64**
8119018	OSL S16 2	S16	15/18	234	37	1.25	0.08	**188**	**32**

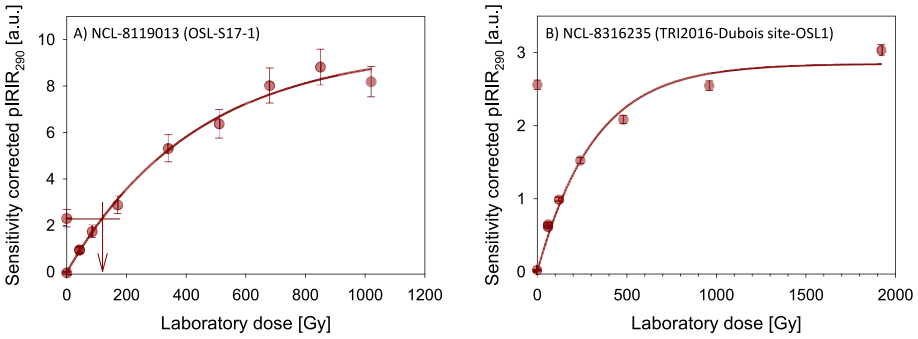

Fig. 9. Typical sensitivity corrected regenerated single aliquot $pIRIR_{290}$ dose response curves (DRCs) are shown for sample OSL-S17-1 (A) and sample TRI2016-Dubois site-OSL1. The dose response data were fitted with a single saturating exponential curve. For A) the sensitivity corrected natural signal plots well below the onset of signal saturation (2D0), i.e. the equivalent dose (D_e) of this aliquot could be determined through interpolation onto the DRC. For B) the sensitivity corrected natural signal plots slightly above the onset of signal saturation ($2D_0$ average of the sample is at 586 Gy), i.e. no D_e could be determined.

grained and probably rapidly deposited BBC-1 characterized by a high deposition rate is slim. Hence, it is most likely that the reversed signal belongs to the Matuyama chron, and thus predates the Brunhes-Matuyama reversal at 773 ± 2 ka (2σ; Channell et al., 2020).

The mostly normal paleomagnetic signal in and above the BBC-2 is interpreted as part of the Brunhes chron. This agrees with the maximum depositional age of 450 ± 110 ka for the BBC-2 based on single grain $^{40}Ar/^{39}Ar$ measurements. As mentioned before, the $^{40}Ar/^{39}Ar$ results indicate that this maximum age of the deposits probably lies close to the actual depositional age. Based on the luminescence-based minimum age of 430 ± 50 ka obtained for the *Pseudodon* shell infills by Joordens et al. (2015), the age of the BBC-2 can be further constrained to 560–380 ka. Importantly, the obtained ages for the BBC-1 and BBC-2 indicate a major depositional hiatus of at least 200 kyr between these two highly fossiliferous units. When placing the newly defined BBC-2 in the revised stratigraphic framework for the Trinil area proposed by Berghuis et al. (2021), the question arises whether the BBC-2 is part of the pre-terrace Batu Gajah Formation, the Trinil Formation, or part of the terrace stratigraphy of the Solo Formation. Based on sedimentological, lithological and fossil content differences with the overlying terrace sediments and similarities with the underlying BBC-1, the BBC-2 is tentatively attributed to the Batu Gajah Formation. Note that the Trinil Fm is absent from the Trinil site left bank site. For a more detailed discussion of the place of the BBC-2 in the revised regional stratigraphic framework see SOM Text 8.

Terrace stratigraphy The unconformable contact between the BBC-2 and the overlying terrace deposits can be seen in both S18B and S19C (SOM Figs. S1B and C). Based on the difference in lithology between the conglomeratic BBC-2 and the overlying finely cross-bedded/laminated sands and silts, this contact is interpreted as the boundary between the pre-terrace Batu Gajah Formation and the terrace-related Solo Formation (Fig. 10). This is supported by the fact that the deposits overlying this boundary are similar in texture and structure to those exposed in sections further west. In the eastern part of the site, at least 5 m of fine-grained Solo Formation deposits overlie the BBC-2, while in the western part of the site these deposits extend down to at least 1.5 m below low-water level (Fig. 10). Towards the top of the section, loose gravel follows with the modern soil on top.

Dating the terrace stratigraphy at Trinil proved difficult, as the three $pIRIR_{290}$ age calculations obtained from the cross-bedded tuffaceous sands in S16 and S17 are of insufficient quality to make any statements regarding their age. Berghuis et al. (2021) ascribe the terrace sediments located at the left bank of the Trinil site to their T2 terrace. We therefore ascribe the sediments at S16 and S17 to this same T2 terrace. The T2 terrace sediments at nearby Grinseng (ca. 800 m west of Trinil) are luminescence dated to 95^{+56}_{-36} ka (Berghuis et al., 2021). The T2 terrace in the Trinil area is tentatively correlated to the Ngangdong terrace in the Kendeng Hills area (Berghuis et al., 2021), situated ca. 15 km to the northeast and dated to 140–92 ka (Rizal et al., 2020).

The correlation between the T2 terrace and the Ngangdong terrace is based on its place in their respective terrace sequence (i.e., the second lowest terrace) and their comparable lithology (well-rounded andesite gravel with reworked carbonate concretions, and tuffaceous sands and silts; see Berghuis et al., 2021 for details). Note that Trinil and the Kendeng Hills areas experienced different tectonic uplift histories, resulting in the Solo river terraces in the two areas now being situated at different elevations. Correlating terraces based on the order in the sequence of terraces should therefore be done with caution due to differences in terrace formation and preservation. For instance, in the Trinil area seven

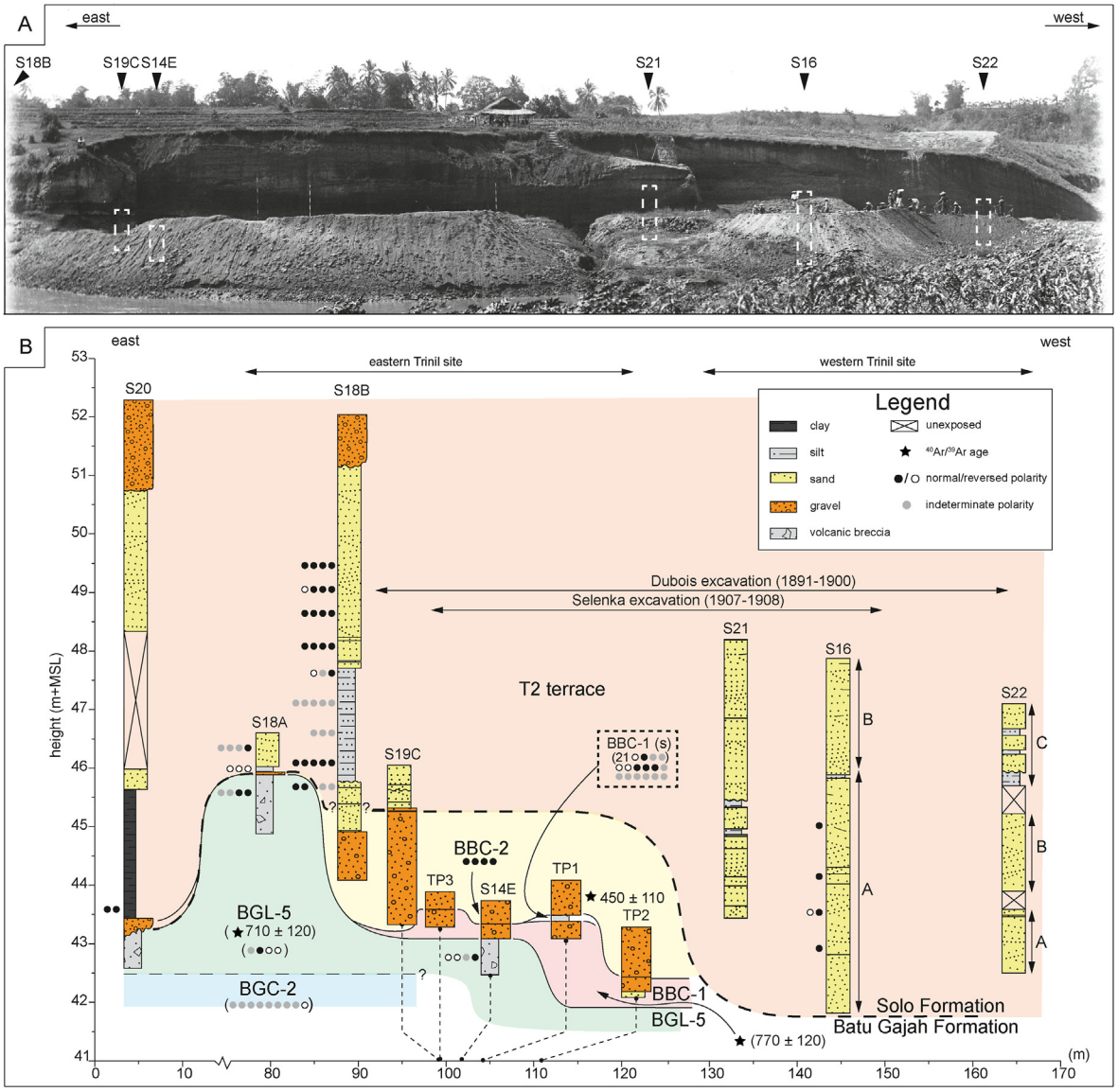

Fig. 10. A) Historic photo (collection number DUBO1399) of the Dubois excavation in 1900, looking south. The approximate locations of the sections are projected onto the historic photograph. B) Stratigraphic framework of the Trinil site with layer names, ages, and formations. All ages are presented in ka. Samples from outcrops are given between brackets. During fieldwork the Solo river water level was around 42.5 m + MSL. Note that the 21 indicates 21 reversed polarity samples in the BBC-1 (s).

terraces are identified (Berghuis et al., 2021) while in the Kendeng area only four terraces are identified (Rizal et al., 2020).

Ultimately the exact age of the T2 terrace deposits at Trinil is of minor importance for this study and although directly dating the terrace sediments at Trinil using pIR-IRSL proved unsuccessful the correlation confirms that the terraces are substantially younger than the BBC-1 and 2. This implies that sediments of a late Middle to Late Pleistocene age are situated at very low elevations in the western part of the Trinil site.

The occurrence of such relatively young deposits at low elevations is unlikely to have been caused by dipping strata—as e.g., suggested by Bartsiokas and Day (1993) based on their interpretation of Carthaus' section drawing (Carthaus, 1911; Tafel VI). Rather, the historical photographs (e.g., Fig. 10A) show that the BBC-1 and BBC-2 channel lag strata exposed in the eastern part of the historical excavation area are intersected by another large channel structure. Sections S21 and S16 expose these fluvial channel deposits, that reach down to at least the base of the visible 1900 back wall and continue until at least 1.5 m below present-day low water level. This deep-cutting channel is likely part of the T2 terrace, as are the deposits that overlie the older pre-terrace strata in the east up to the gravel in the top of S18B.

4.2. Comparison with previous stratigraphic and dating studies

When comparing the new stratigraphic framework presented in this paper with those of Dubois and Selenka, some interesting observations can be made. The presence of a marine breccia at the base of Dubois' stratigraphy (G; Fig. 11A) strongly indicates its composite nature; such deposits can only be found ca. 900 m northwest of the Trinil site (Pengkol and Padas Malang; Fig. 1C). Dubois' claystone (F) is most likely the BGC-2, the lowest unit observed at the Trinil left-bank site (then and during our fieldwork). Above that, Dubois indicates a conglomerate (E) which could either be BGL-5 deposits that thins out going west (see e.g., Fig. 10B), or BBC-1 deposits directly overlying the BGC-2. As Dubois

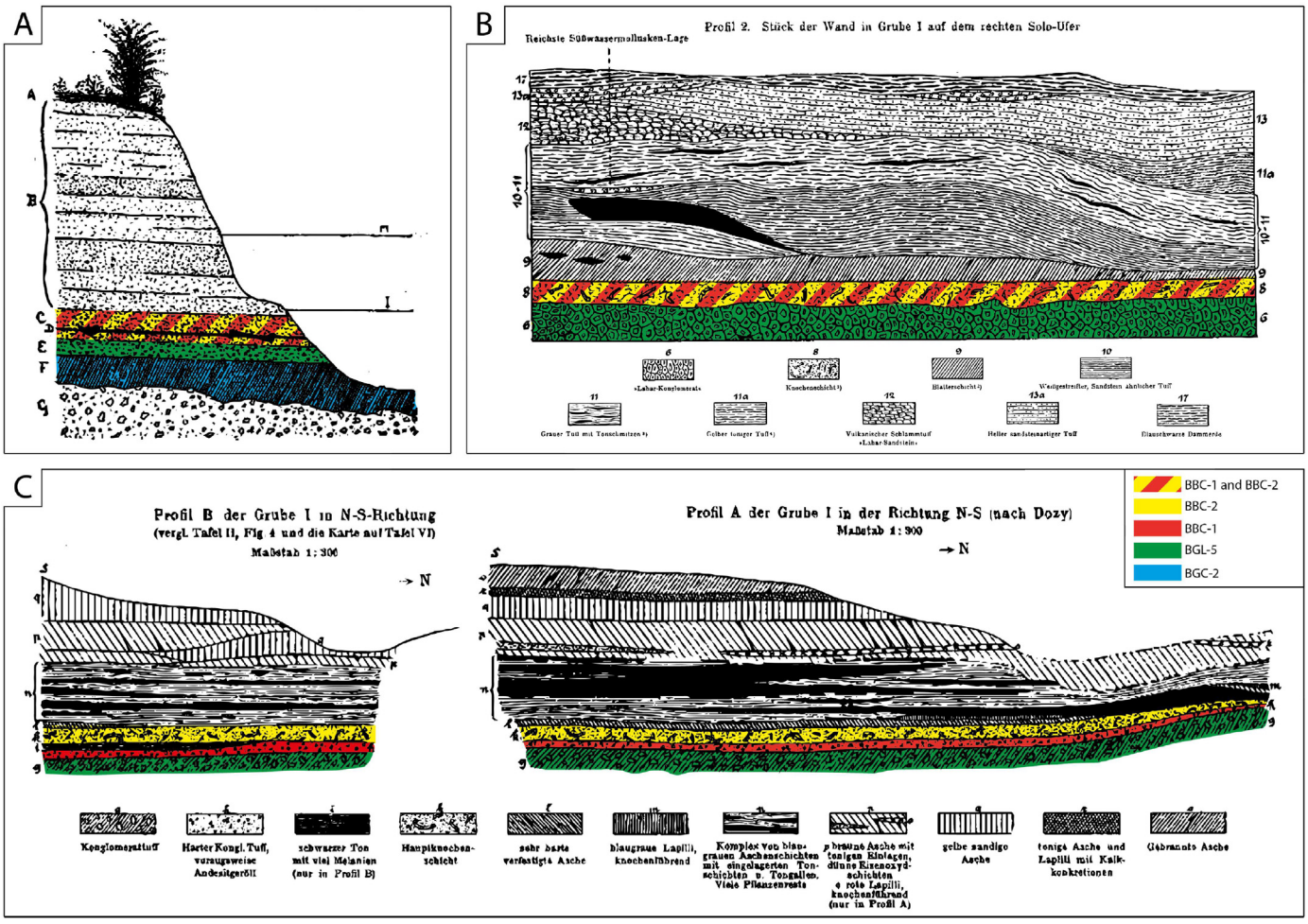

Fig. 11. Trinil stratigraphy of A) Dubois (1896), B) Carthaus (1911), and C) Dozy (1911). Notice how a single fossiliferous layer is drawn by Dubois (layer c = lapilli layer) and by Oppenoorth and Carthaus (layer 8 = Knochenschicht), while Dozy distinguishes two fossiliferous layers (h = Harter Konglomerat Tuff and k = Hauptknochenschicht) occasionally separated by a black clay (layer i). Note that Dubois' 'layer' D is the hominin fossil find horizon and not a separate layer.

describes the conglomerate as only rarely yielding fossils, it is most likely that these are BGL-5 deposits. This would imply that his fossil-rich lapilli layer (C) includes both the BBC-1 and BBC-2. Note that Dubois' hominin fossil find horizon (D) is located within the lapilli layer. This lack of distinction between the two fossiliferous layers is supported by the written documentation, including Dubois' correspondence with his field staff, which makes no mention of multiple find-rich levels. Dubois' lapilli layer is overlain by a soft sandstone (B) that was also observed during our fieldwork in a similar position and is interpreted as T2 terrace sediments. Dubois' stratigraphy is capped by a topsoil (A).

Carthaus (1911) described a stratigraphic sequence for the right river bank, with a single 'Knochenschicht' overlying a lahar conglomerate (Fig. 11B). Oppenoorth however describes but does not illustrate the 'Knochenschicht' as tripartite with a fining up sequence, with the lowermost part being a coarse conglomerate (Oppenoorth, 1911). Dozy (1911) drew two fossiliferous layers in his stratigraphy (Fig. 11C): a lower, coarser, fossiliferous conglomerate ('Harter Konglomerattuff'), followed by the main bone bed ('Hauptknochenschicht'), emphasizing the presence of two highly fossiliferous layers. The coarse conglomerate at the base of both Oppenoorth's and Dozy's stratigraphy corresponds accurately with the BBC-1, while the upper, finer fossiliferous part (s), corresponds best to the BBC-2. In conclusion, Dubois and Carthaus appear to have made no distinction between the two highly fossiliferous layers that are present at the site, while Dozy and Oppenoorth did.

Furthermore, any reference to younger deposits resulting from fluvial incisions (i.e., T2 and younger deposits) situated at low water level appears to be absent from the historical documentation by Dubois as well as Selenka. However, the presence of late Middle to Late Pleistocene terrace deposits at the Trinil site and their contribution to the Trinil fossil assemblage has already been suggested by Bartstra (1982) and is supported by the results presented in this paper.

Despite decades of discussion regarding the Trinil sites to do chronology and fauna, available ages are limited. An age estimate of ca. 0.9 Ma for the Trinil fossil assemblage is based on the faunal similarities between Trinil and the Grenzbank level in Sangiran combined with absolute ages for the latter. Despite the much younger absolute ages presented for sediments within fossil *Pseudodon* shells from the Trinil site (Joordens et al., 2015) that are incompatible with those based on the correlation with the Grenzbank at Sangiran, this age of ~0.9 Ma is still being used to date Trinil fossils (e.g., van der Geer et al., 2018; Volmer et al., 2019). The ages presented in the current study demonstrate that the fossil-rich strata at Trinil are dated at 830–773 ka and at 560–380 ka, younger than the ~0.9 Ma previously proposed based on the biostratigraphic correlation with the Grenzbank (Fig. 12).

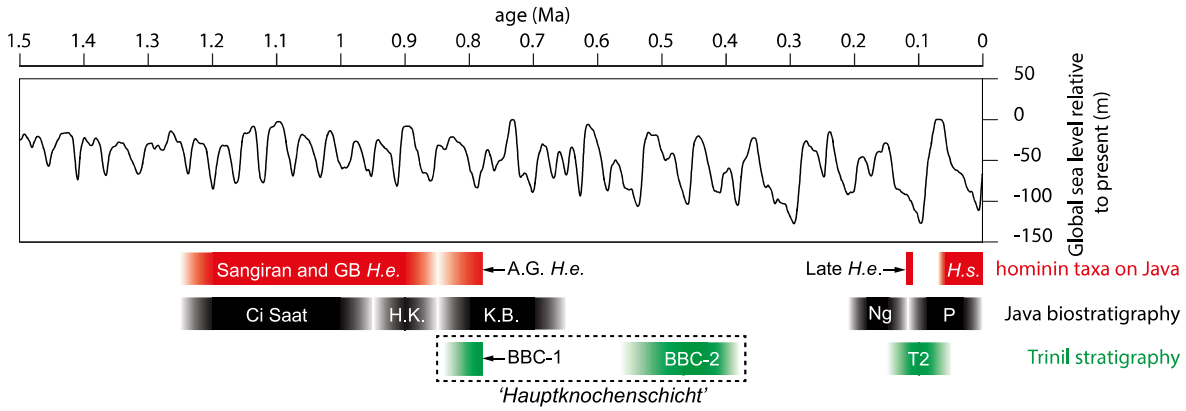

Fig. 12. Chronological overview of Java's biostratigraphy and hominin fossil record, and Trinil (chrono)stratigraphy presented next to the benthic $\delta^{18}O$ stack (Lisiecki and Raymo, 2005). Red blocks indicate hominin taxa on Java: Sangiran and GB H. e. = *Homo erectus* in Sangiran Formation and Grenzbank; AG H. e. = *H. erectus* above Grenzbank (Kaifu et al., 2010); Late H. e = Late *H. erectus* (Kaifu et al., 2010; Rizal et al., 2020); H.s. = *Homo sapiens* (O'Connell et al., 2018). Black blocks indicate Java biostratigraphy: Ci Saat = Ci Saat fauna, H.K. = Trinil H.K. fauna, KB = Kedung Brubus fauna, Ng = Ngangdong fauna, P = Punung fauna (Van den Bergh et al., 2001; Westaway et al., 2007; Matsu'ura et al., 2020; Rizal et al., 2020). Green blocks indicate Trinil stratigraphy: BBC-1 = Bone Bearing Channel 1; BBC-2 = Bone Bearing Channel 2; T2 = terrace T2; (ages the correlation with the Ngangdong terrace by Berghuis et al., 2021). Note that the BBC-1 contains faunal and hominin fossils associated with the Trinil H.K. fauna and Sangiran/GB *Homo erectus* group, instead of the Kedung Brubus fauna and Bapang/AG *H. erectus* group which would be expected (providing there is no reworking) based on the chronological age model for Trinil deposits presented in this paper. Note also the multiple long hiatuses in the Trinil stratigraphy.

4.3. The potential role of reworking in the fossil-rich strata

When discussing the discrepancy between the age estimates based on biostratigraphic arguments and the chronostratigraphic age model presented here, it should be noted that the latter only resolves the age of the deposits in which fossils were found, not the age of the fossils themselves. Sediments and fossils deposited in fluvial contexts are often influenced by reworking. At Trinil, we have evidence for repeated fluvial erosion and deposition with each channel cutting through older ones and reworking its fossil content. The $^{40}Ar/^{39}Ar$ data presented here and in Joordens et al. (2015) provide evidence for this; samples from individual layers provide a continuous record of $^{40}Ar/^{39}Ar$ ages reaching back to as early as ~2.5 Ma—i.e., similar in age to the oldest radioisotope ages available for Pleistocene Java (e.g., Larick et al., 2001). Whether the fluvial processes were also able to transport heavier components depends on the energy levels involved. The BBC-1 and BBC-2 are poorly sorted conglomerates, with a certain amount of gravel-sized material. Particularly the BBC-1 contains large, rounded cobbles and boulders up to 1 m in diameter (SOM Fig. S4B), suggesting substantial transport energy and/or the formation of lag deposits. They likely originate from the underlying BGL-5, in which clasts of similar shape and size can be found. Furthermore, both the BBC-1 and BBC-2 contain pebble to cobble-sized clasts with different shapes and degrees of rounding (ranging from angular to rounded) in various stages of weathering, suggesting heterogeneity in the source area and transportation time/distance. This suggests that there probably has been sufficient energy to transport and rework mineralized bones.

Although the fossil material recovered during our fieldwork was limited, several observations—also found in the historical documentation—support the notion of reworked fossils. First, no fossils have been found in anatomical connection in the BBC-1 and 2, neither during our excavation nor has it been reported for the H.K. from the historical excavations (Carthaus, 1911). Secondly, the excavated fossils show heterogeneous surface taphonomy likely indicative of heterogenous fossilization conditions, which may point to different sources both in origin and age. However, the material we excavated was situated near the surface (<1 m deep), exposing it to various levels of oxidation and repeated wetting and drying. Therefore, it may not be representative of the material excavated from a larger depth, as was frequently the case with the historical excavations. Thirdly, the excavated fossils and those found in the historical museum collections from Trinil are heavily fossilized. In general, more mineralized bones are more brittle than less mineralized bones, and therefore more prone to breakage (Currey, 1984; Lyman and Lyman, 1994). This suggests that the material excavated from the test pits, which consists mostly of fragments, probably was fossilized before transportation and deposition. An argument for limited transport is the lack of surface abrasion (Blanckenhorn, 1911; Dozy, 1911; Carthaus, 1911), but this also depends on the state of mineralization (i.e., fresh or fully fossilized/mineralized; see above) of the fossils upon transport and transport path length.

Although a systematic analysis is necessary to understand the taphonomic history of the fossil assemblages from Trinil, it is clear that the processes involved in the deposition of the most find-rich strata had sufficient energy to erode and rework fossilized bones and that, based on preliminary observations, transport of vertebrate fossils is likely.

For one particular type of fossil, the fossil *Pseudodon* shells, significant transport can be excluded. The shells found during our excavation in both the BBC-1 and BBC-2 include many complete specimens (SOM Fig. S4D), some of which had both valves still connected. This is also true for those from the Dubois collection, of which one specimen carried the famous zigzag line interpreted as the earliest evidence of an intentional abstract engraving by hominins (Joordens et al., 2015). These shells can therefore be considered contemporaneous with the deposits in which they were found.

4.4. Implications for the Trinil (H.K.) fauna including the hominin remains

The results of the chronostratigraphic framework presented here point to a substantially more complex stratigraphy than is reflected in the initial schematic drawings by Dubois. Deposits ranging in age from Early Pleistocene (BGL-5, BBC-1), Middle Pleistocene (BBC-2), and potentially even late Middle to Late Pleistocene (T2 terrace) are present at Trinil. More critically, all these deposits can be encountered at a similar stratigraphic height, at the low-water levels where the excavations of Dubois and

Selenka focused on. The historical documentation shows that the fossil-rich, but very differently aged BBC-1 and BBC-2 were the main target(s) of the historical excavations and that Dubois and Carthaus did not distinguish between the two layers. Finally, for all these deposits, but particularly for the BBC-1 and BBC-2, the reworking of (fossil) material is likely. These findings have far-reaching implications for the interpretation of the historical collections and the conclusions drawn from them. Here, in particular, we discuss the implications for the Trinil H.K. fauna and the Javanese biostratigraphy.

Dubois originally defined his fossil assemblage from Trinil and other nearby localities as the 'Kendeng' or 'Trinil fauna' (Dubois, 1907, 1908). Almost 75 years later, doubt regarding the unity of this fauna led to the definition of the Trinil H.K. fauna, which was specified to only include fossils from a known stratigraphic context (de Vos et al., 1982; Sondaar, 1984). These authors claimed that, based on the Dubois' (very limited) provenance information, all fossils in their faunal species list (see Table 1 in de Vos, 1989) came from a single bone bed situated at low water level, the 'Hauptknochenschicht' (de Vos and Sondaar, 1982; de Vos 1984; Ingicco et al., 2014). This assessment allowed the authors to use the Trinil H.K. fauna as a unit in their revised biostratigraphy of Java. However, our results demonstrate that at the Trinil site there are at least three fossiliferous units situated at low water level, the BBC-1, BBC-2, and T2 deposits instead of a single, homogenous bone bed.

In addition, this complicates the assumed age of the Trinil H.K. fauna of ca. 0.9 Ma based on the biostratigraphic correlation with the well-dated Grenzbank level in Sangiran (Leinders et al., 1985; van den Bergh et al., 1996; Saleki et al., 1998; Matsu'ura et al., 2020) as the age of the fossil-rich deposits at Trinil appears to be (slightly) younger. The most straightforward explanation for this discrepancy is that the material was, at least partially, reworked from older deposits (i.e., of Grenzbank-equivalent or older age). Reworking from deposits similar in age to the Grenzbank would also explain the similarity in fluorine content—despite inherent shortcoming of this method (e.g., Tankersley and Wells, 2011)—between fossils from Trinil and the Grenzbank at Sangiran (Matsu'ura, 1986), while the fluorine content of fossils from the overlying Bapang Formation at Sangiran is significantly lower. Following this line of argumentation, the fact that the fluorine content of some Trinil specimens in the Dubois collection does fall within the range of the younger Middle Pleistocene Bapang Formation material may point to a (limited) contribution of Late to Middle Pleistocene fossil material to the Dubois Collection.

Furthermore, the Trinil 2 skullcap is morphologically similar to the specimens from the Grenzbank and the underlying upper Sangiran Formation at Sangiran (Kaifu et al., 2010; Kaifu, 2017) dated to between ~1.3 and ~0.9 Ma (Matsu'ura et al., 2020), older than 1.51 ± 0.08 Ma (2σ, Larick et al., 2001), or even ~1.8 Ma (Husson et al., 2022). This is in stark contrast with the ages obtained for the highly fossiliferous BBC-1 and BBC-2 at Trinil dated in this study at 830–773 and 560–380 ka, respectively. Based on these chronological constraints at the Trinil site, one would expect more similarity with the *H. erectus* specimens from the Bapang Formation above the Grenzbank (Bapang AG), which date between ~0.9 and 0.773 Ma based radioisotopic measurements and the location of the Brunhes-Matuyama reversal (Fig. 12; Hyodo et al., 2011; Matsu'ura et al., 2020). This apparent discrepancy could also be explained by a reworking scenario where the Trinil 2 skullcap is reworked from older deposits.

Apart from taxa that are generally known from contexts older than our new age model, the Trinil H.K. fauna also contains elements that so far have been found only in settings younger than the depositional ages of the BBC-1 and BBC-2. For example, the Gibbon (Hylobatidae)—represented at Trinil by a femur that is claimed to represent the oldest occurrence of this species in Insular SE Asia (Ingicco et al., 2014)—is generally associated with the Late Pleistocene Punung fauna (Storm et al., 2005; Westaway et al., 2007; Jablonski and Chaplin, 2009). Other Trinil H.K. elements that are not known from either Early or Middle Pleistocene sediments in SE Asia are leopard cat (*Prionailurus [=Felis] bengalensis*), Malayan porcupine (*Hystrix brachyura*), and silvery langur ('*Presbytatis*' *[=Trachypithecus] cristatus*; van den Bergh et al., 1996). Some also consider the hominin Femur I as an outlier, for instance, Ruff et al. (2015) pointed out that based on morphological grounds, Femur I would fit comfortably within Late Pleistocene *Homo* while showing no attributes typical of early *Homo* femora. The terrace deposits with a late Middle to Late Pleistocene age are a likely source for these potentially substantially younger fossils.

Based on the presence of these relatively young taxa, it is necessary to reconsider the Trinil H.K. fauna, which probably is a time averaged assemblage as already suspected by Bartstra (e.g. 1978, 1982). Direct dating of fossils from Trinil might provide further evidence as to the degree of reworking at Trinil and the heterogeneity of the Trinil fossil assemblage.

5. Conclusions

In this paper, we present a revised stratigraphic framework for the Trinil site which is embedded within the stratigraphic framework of the larger Trinil area. A comparison of our new fieldwork-based data with previous litho-, chrono- and biostratigraphic studies reveals a complex stratigraphy with significant hiatuses. Combined with the reworked nature of the deposits and the limited primary excavation documentation, this potentially has major implications for the hominin and faunal fossils of the historical Dubois and Selenka collections from Trinil.

At the Trinil site, Early, Middle and potentially even late Middle to Late Pleistocene fossiliferous layers are present at the low-water levels on which the historical excavations led by Dubois and Selenka focused. Two of these are highly fossiliferous layers, the BBC-1 and BBC-2, and represent two separate conglomeratic channel fills. The lower fossiliferous layer, the BBC-1, has an age of 830–773 ka. The upper fossiliferous layer, the BBC-2, is substantially younger with an age range of 560–380 ka. Furthermore, (significantly) younger terrace deposits are present at the Trinil site at similar elevations. As such, the chronological framework presented in this study suggests the presence of at least two major hiatuses in the Trinil site stratigraphy.

Concerning the historic excavations, Dubois' 'Lapillischicht' and Carthaus' 'Knochenschicht' likely constitute two separate fossiliferous layers, BBC-1 and BBC-2, while Dozy correctly distinguished between them. This implies that the historical collections from Trinil are a mix of fossils from differently-aged units that likely contain reworked fossil material of varying ages. As such, based on the present study it is not possible to assign absolute ages to the specific fossils.

We propose a scenario in which the Trinil H.K. fauna is influenced by reworking of fossils of various ages. This scenario might explain why the Trinil skullcap collected by Dubois is tentatively grouped with Sangiran *Homo erectus* fossils aged 1.3–0.9 Ma based on morphology, while other hominin fossils (like Femur I) share affinities with *Homo* fossils of late Pleistocene age. Further research is needed to test this scenario, preferably by applying direct dating on the fossil assemblage from Trinil, together with an extensive taphonomic analysis of the fossils in the historic collections and those collected during fieldwork. This might lead to a better constrained 'Trinil fauna'.

Author contributions

TS, JJ, and SA conceived and designed the project. JJ aquired the funding. SH, SA, EP, TV, TS, HB and JJ conceptualized the research. BP, SA, DRE, MH and TS ensured embedding in the Indonesian research infrastructure, and MH and DRE conducted project and fieldwork administration. SH, EP, SA, MH, IS, DY, TR, HB, TV, DRE, AV, GA, OD, RB, MH and JJ participated in the fieldwork, that was overall supervised by SA and JJ. EP, SA and AV directed the excavations. IS, OD and GA excavated, curated and analyzed faunal fossils. SH, TV, DY, HB, HV, EP, RB and JJ did the geological investigation and analysis. SH and KK conducted the Ar/Ar dating. SH, DY, GD-N, WK and NN measured and interpreted the paleomagnetic samples. SH and TR conducted the luminescence dating. SH designed the figures and wrote the manuscript with EP, KK, SA and JJ. All authors contributed to the writing, review and editing of the manuscript.

Declaration of competing interest

The authors declare that they have no known competing financial interests or personal relationships that could have appeared to influence the work reported in this paper.

Data availability

The data that has been used is confidential.

Acknowledgments

This study was carried out with the permission of the Indonesian Ministry of Research, Technology and Higher Education (RISTEK research permits: 263/SIP/FRP/ES/Dit.KI/VII/2016, 33/SIP/FRP/E5/Dit.KI/II/2018 and 12/E5/E5.4/SIP.EXT/2019 of Josephine Joordens; 8 B/TKPIPA/E5/Dit.KI/VIII/2018 and 2/TKPIPA/E5/Dit.KI/II/2019 of Sander Hilgen) under the project 'Studying Human Origin in East Java'. We thank Arkenas (Pusat Penelitian Arkeologi Nasional) and in particular Dr. I Made Geria, Priyatno Hadi Sulistyarto, and Marlon Ririmasse for facilitating and supporting our collaborative research. We would also like to thank BPCB Jawa Timur and the Government Regency of Ngawi for giving us support and permission to do research in Trinil. We are grateful to the people of Trinil, Kawu and Ngancar and the staff of the Trinil Museum for their hospitality and support. We thank our 2016, 2018 and 2019 fieldwork teams, notably collaborators and assistants Catur Hari Gumono, Agus Hadi Widianto and Suwono, and the Gadjah Mada University students Triastuti Puji Hapsari, Abdul Aziz and Nadia Shafira. We acknowledge Frank Huffman's contributions to the 2016 fieldwork campaign and the planning of the 2017–2019 fieldwork campaign. Alice Versendaal and Roel van Elsas are thanked for their technical support in the lab. The research was funded by the Treub Foundation (Maatschappij voor Wetenschappelijk Onderzoek in de Tropen), SNMAP (Stichting Nederlands Museum voor Anthropologie en Praehistorie), the Faculty of Archaeology, Leiden University, and the Dutch Research Council NWO (Grant number 016. Vidi.171.049 to Joordens).

Appendix A. Supplementary data

Supplementary data to this article can be found online at https://doi.org/10.1016/j.quascirev.2022.107908.

References

Bartsiokas, A., Day, M.H., 1993. Electron probe energy dispersive X-ray microanalysis (EDXA) in the investigation of fossil bone: the case of Java man. Proceedings. Biological sciences 252, 115–123. https://doi.org/10.1098/rspb.1993.0054.

Bartstra, G.-J., 1978. The age of the Djetis beds in East and central Java. Antiquity 52, 56–58.

Bartstra, G.-J., 1982. The river-laid strata near Trinil, site of *Homo erectus* Java, Indonesia. Mod. Quat. Res. Southeast Asia 7, 97–130.

Berghuis, H.W.K., Veldkamp, A., Adhityatama, S., Hilgen, S.L., Sutisna, I., Barianto, D.H., Pop, E.A., Reimann, T., Yurnaldi, D., Ekowati, D.R., 2021. Hominin homelands of East Java: revised stratigraphy and landscape reconstructions for plio-pleistocene Trinil. Quat. Sci. Rev. 260, 1–27. https://doi.org/10.1016/j.quascirev.2021.106912.

Blanckenhorn, M., 1911. Allgemeine Betrachtungen der wissenschaftlichen Ergebnisse der Selenka-Trinil Expedition. In: Selenka, L., Blanckenhorn, M. (Eds.), Die *Pithecanthropus*-Schichten Auf Java. Geologische Und Paläontologische Ergebnisse Der Trinil-Expedition (1907 Und 1908). Verlag Von Wilhelm Engelmann, Leipzig, pp. 256–268.

Buylaert, J.-P., Jain, M., Murray, A.S., Thomsen, K.J., Thiel, C., Sohbati, R., 2012. A robust feldspar luminescence dating method for Middle and Late Pleistocene sediments. Boreas 41, 435–451. https://doi.org/10.1111/j.1502-3885.2012.00248.x.

Carthaus, E., 1911. Zur geologie von Java. In: Selenka, L., Blanckenhorn, M. (Eds.), Die Pithecanthropus-Schichten Auf Java. Geologische Und Paläontologische Ergebnisse Der Trinil-Expedition (1907 Und 1908). Verlag Von Wilhelm Engelmann, Leipzig, pp. 1–33.

Channell, J.E.T., Singer, B.S., Jicha, B.R., 2020. Timing of Quaternary geomagnetic reversals and excursions in volcanic and sedimentary archives. Quat. Sci. Rev. 228, 1–28. https://doi.org/10.1016/j.quascirev.2019.106114.

Currey, J.D., 1984. Effects of differences in mineralization on the mechanical properties of bone. Phil. Trans. Roy. Soc. Lond. B Biol. Sci. 304, 509–518.

de Vos, J., 1989. The environment of *Homo erectus* from Trinil H.K. Proceedings of the 2 nd.

de Vos, J.,1984. Reconsideration of Pleistocene cave faunas from South China and their relation to the faunas from Java. Cour. Forsch.-Inst. Senckenberg 69, 259–266.

de Vos, J., Aziz, F., 1989. The excavations by Dubois (1891-1900), Selenka (1906-1908), and the geological survey by the Indonesian-Japanese team (1976-1977) at Trinil (Java, Indonesia). J. Anthropol. Soc. Nippon 97, 407–420. https://doi.org/10.1537/ase1911.97.407.

de Vos, J., Sondaar, P.Y., 1982. The importance of the "Dubois Collection" reconsidered. Mod. Quat. Res. Southeast Asia 7, 35–63.

de Vos, J., Sartono, S., Hardja-Sasmita, S., Sondaar, P.Y., 1982. The fauna from Trinil, type locality of *Homo erectus*: a reinterpretation. Geol. Mijnbouw 61, 207–211.

Dozy, C.M., 1911. Bemerkungen zur Stratigraphie der Sedimente in der Triniler Gegend. In: Selenka, L., Blanckenhorn, M. (Eds.), Die *Pithecanthropus*-Schichten Auf Java. Geologische Und Paläontologische Ergebnisse Der Trinil-Expedition (1907 Und 1908). Verlag Von Wilhelm Engelmann, Leipzig, pp. 34–36.

Dubois, E., 1894. *Pithecanthropus erectus*: eine menschenähnliche Übergangsform aus Java. Landesdruckerei, Batavia.

Dubois, E., 1895. *Pithecanthropus erectus*, betrachtet als eine wirkliche Übergangsform und als Stammform des Menschen, Zeitschrift für Ethnologie. Z. Ethnol.

Dubois, E., 1896. On *Pithecanthropus erectus*: a transitional form between man and the apes. J. Anthropol. Inst. G. B. Ireland 25, 240–255.

Dubois, E., 1899. Abstract of remarks upon the brain-cast of *Pithecanthropus erectus*. Journal of Anatomy and Physiology 33, 273–276.

Dubois, E., 1907. Eenige van Nederlandschen kant verkregen uitkomsten met betrekking tot de kennis der Kendeng-fauna (fauna van Trinil). Tijdschrift van het Koninklijk Nederlandsch Aardrijkskundig Genootschap 24 (2), 449–458.

Dubois, E., 1908. Das geologische alter der Kendeng-oder trinil-fauna. Tijdschrift van Het Koninklijk Nederlandsch Aardrijkskundig Genootschap 25 (2), 1235–1270.

Dubois, E., 1932. De Afzonderlijk Organisatie van *Pithecanthropus* waarvan het Femur Getuigt, thans bevestigd door andere individuen van de beschreven soort. Verslag van de gewone vergaderingen der afdeeling natuurkunde. Koninklijke Akademie van Wetenschappen te Amsterdam 41, 76–77.

Dubois, E., 1934. New evidence of the distinct organization of Pithecanthropus. Proceedings of the Section of Sciences of the Koninklijke Akademie van Wetenschappen 37, 139–145.

Duyfjes, J., 1936. Zur geologie und stratigraphie des Kendenggebietes zwischen Trinil und Soerabaja (Java). De Ingenieur ned.-Indië 4, 136–149.

Guérin, G., Mercier, N., Adamiec, G., 2011. Dose-rate conversion factors: update. Ancient Tl 29 (1), 5–8.

Hepburn, D., 1896. The Trinil femur (*Pithecanthropus erectus*), contrasted with the femora of various savage and civilised races. Journal of anatomy and physiology 31, 1.

Husson, L., Salles, T., Lebatard, A.E., Zerathe, S., Braucher, R., Noerwidi, S., Aribowo, S., Mallard, C., Carcaillet, J., Natawidjaja, D.H., Bourlés, D., ASTER team, 2022. Javanese Homo erectus on the move in SE Asia circa 1.8 Ma. Sci. Rep. 12, 19012. https://doi.org/10.1038/s41598-022-23206-9.

Hyodo, M., Matsu'ura, S., Kamishima, Y., Kondo, M., Takeshita, Y., Kitaba, I., Danhara, T., Aziz, F., Kurniawan, I., Kumai, H., 2011. High-resolution record of the Matuyama-Brunhes transition constrains the age of Javanese *Homo erectus* in the Sangiran dome, Indonesia. Proc. Natl. Acad. Sci. U. S. A 108, 19563–19568. https://doi.org/10.1073/pnas.1113106108.

Ingicco, T., de Vos, J., Huffman, O.F., 2014. The oldest gibbon fossil (hylobatidae) from insular Southeast Asia: evidence from Trinil,(East Java, Indonesia), lower/

middle Pleistocene. PLoS One 9, 1–15. https://doi.org/10.1371/journal.pone.0099531.g004.
Jablonski, N.G., Chaplin, G., 2009. The fossil record of gibbons. In: Whittaker, D., Lappan, S. (Eds.), The Gibbons: New Perspectives on Small Ape Socioecology and Population Biology, Developments in Primatology: Progress and Prospects. Springer, New York, NY, pp. 111–130. https://doi.org/10.1007/978-0-387-88604-6_7.
Joordens, J.C.A., d'Errico, F., Wesselingh, F.P., Munro, S., de Vos, J., Wallinga, J., Ankjærgaard, C., Reimann, T., Wijbrans, J.R., Kuiper, K.F., Mücher, H.J., Coqueugniot, H., Prié, V., Joosten, I., van Os, B., Schulp, A.S., Panuel, M., van der Haas, V., Lustenhouwer, W., Reijmer, J.J.G., Roebroeks, W., 2015. *Homo erectus* at Trinil on Java used shells for tool production and engraving. Nature 518, 228–231. https://doi.org/10.1038/nature13962.
Kaifu, Y., 2017. Archaic hominin populations in Asia before the arrival of modern humans: their phylogeny and implications for the "southern denisovans. Curr. Anthropol. 58, 418–433. https://doi.org/10.1086/694318.
Kaifu, Y., Indriati, E., Aziz, F., Kurniawan, I., Baba, H., 2010. Cranial morphology and variation of the earliest Indonesian hominids. In: Norton, C.J., Braun, D.R. (Eds.), Asian Paleoanthropology: from Africa to China and beyond, Vertebrate Paleobiology and Paleoanthropology. Springer Netherlands, Dordrecht, pp. 143–157. https://doi.org/10.1007/978-90-481-9094-2_11.
Koymans, M., Langereis, C., Pastor-Galán, D., 2016. Paleomagnetism.org: an online multi-platform open source environment for paleomagnetic data analysis. Comput. Geosci. 93, 127–137. https://doi.org/10.1016/j.cageo.2016.05.007.
Kuiper, K.F., Deino, A., Hilgen, F.J., Krijgsman, W., Renne, P.R., Wijbrans, J.R., 2008. Synchronizing rock Clocks of Earth history. Science 320, 500–504. https://doi.org/10.1126/science.1154339.
Larick, R., Ciochon, R.L., Zaim, Y., Sudijono, Suminto, Rizal, Y., Aziz, F., Reagan, M., Heizler, M., 2001. Early Pleistocene 40Ar/39Ar ages for Bapang Formation hominins, central Jawa, Indonesia. Proc. Natl. Acad. Sci. USA 98, 4866–4871. https://doi.org/10.1073/pnas.081077298.
Leinders, J.J.M., Aziz, F., Sondaar, P.Y., de Vos, J., 1985. The age of the hominid-bearing deposits of Java; state of the art. Geol. Mijnbouw 64, 167–173.
Lisiecki, L.E., Raymo, M.E., 2005. A Pliocene-Pleistocene stack of 57 globally distributed benthic δ18O. records. Paleoceanography 20. https://doi.org/10.1029/2004PA001071.
Lyman, R.L., Lyman, C., 1994. Vertebrate Taphonomy. Cambridge University Press.
Madsen, A.T., Murray, A.S., Andersen, T.J., Pejrup, M., Breuning-Madsen, H., 2005. Optically stimulated luminescence dating of young estuarine sediments: a comparison with 210Pb and 137Cs dating. Marine Geology 214, 251–268. https://doi.org/10.1016/j.margeo.2004.10.034.
Manouvrier, L., 1895. Discussion sur le "*pithecanthropus erectus*" comme précurseur présumé de l'homme. Bull. Mem. Soc. Anthropol. Paris 6, 12–47.
Matsu'ura, S., 1986. Fluorine and phosphate analysis of fossil bones from the Kabuh Formation of Trinil. Bulletin of the National Science Museum, Tokyo, Series D (Anthropology) 12, 1–9.
Matsu'ura, S., Kondo, M., Danhara, T., Sakata, S., Iwano, H., Hirata, T., Kurniawan, I., Setiyabudi, E., Takeshita, Y., Hyodo, M., Kitaba, I., Sudo, M., Danhara, Y., Aziz, F., 2020. Age control of the first appearance datum for Javanese *Homo erectus* in the Sangiran area. Science 367, 210–214. https://doi.org/10.1126/science.aau8556.
Mayr, E., 1944. On the concepts and terminology of vertical subspecies and species. National research Council committee on common problems of genetics. Paleontology, and Systematics Bulletin 2, 11–16.
Mayr, E., 1950. Taxonomic categories in fossil hominids. In: Cold Spring Harbor Symposia on Quantitative Biology. Cold Spring Harbor Laboratory Press, pp. 109–118.
Meikle, W.E., Parker, S.T., 1994. Naming Our Ancestors: an Anthology of Hominid Taxonomy. Waveland Press Inc.
Oppenoorth, W.F.F., 1911. Arbeitsbericht uber die Ausgrabungen. I. Teil. Die Arbeiten des Jahres 1907 bis August. In: Selenka, L., Blanckenhorn, M. (Eds.), Die Pithecanthropus Schichten Auf Java, Geologische Und Palaeontologische Ergebnisse Der Trinil-Expedition (1907-1908). W. Engelmann, Leipzig Leipzig (XXVI–XXXVIII).
Min, K., Mundil, R., Renne, P.R., Ludwig, K.R., 2000. A test for systematic errors in 40Ar/39Ar geochronology through comparison with U/Pb analysis of a 1.1-Ga rhyolite. Geochimica et Cosmochimica Acta 64 (1), 73–98. https://doi.org/10.1016/S0016-7037(99)00204-5.
O'Connell, J.F., Allen, J., Williams, M.A.J., Williams, A.N., Turney, C.S.M., Spooner, N.A., Kamminga, J., Brown, G., Cooper, A., 2018. When did *Homo sapiens* first reach Southeast Asia and Sahul? Proc. Natl. Acad. Sci. USA 115, 8482–8490. https://doi.org/10.1073/pnas.1808385115.
Prescott, J.R., Hutton, J.T., 1994. Cosmic ray contributions to dose rates for luminescence and ESR dating: large depths and long-term time variations. Radiation measurements 23, 497–500.
Rizal, Y., Westaway, K.E., Zaim, Y., van den Bergh, G.D., Bettis, E.A., Morwood, M.J., Huffman, O.F., Grün, R., Joannes-Boyau, R., Bailey, R.M., Sidarto Westaway, M.C., Kurniawan, I., Moore, M.W., Storey, M., Aziz, F., Suminto Zhao, J., Aswan Sipola, M.E., Larick, R., Zonneveld, J.-P., Scott, R., Putt, S., Ciochon, R.L., 2020. Last appearance of *Homo erectus* at Ngandong, Java, 117,000–108,000 years ago. Nature 577, 381–385. https://doi.org/10.1038/s41586-019-1863-2.
Rogers, R.R., Kidwell, S.M., 2007. A conceptual framework for the genesis and analysis of vertebrate skeletal concentrations. In: Rogers, R.R., Eberth, D.A., Fiorillo, A.R. (Eds.), Bonebeds: Genesis, Analysis, and Paleobiological Significance. The University of Chicago Press, pp. 1–65.
Ruff, C.B., Puymerail, L., Macchiarelli, R., Sipla, J., Ciochon, R.L., 2015. Structure and composition of the Trinil femora: functional and taxonomic implications. J. Hum. Evol. 80, 147–158. https://doi.org/10.1016/j.jhevol.2014.12.004.
Saleki, H., Féraud, G., Sémah, F., Falguères, C., Sémah, A.M., Djubiantono, T., 1998. Datations radiométriques des couches à *Homo erectus* de Kabuh à Ngebung (Sangiran, Java central, Indonésie). Actes du XIIIe Congrès UISPP Forli Italie 2, 63–74.
Schaen, A.J., Jicha, B.R., Hodges, K.V., Vermeesch, P., Stelten, M.E., Mercer, C.M., Phillips, D., Rivera, T.A., Jourdan, F., Matchan, E.L., 2020. Interpreting and reporting 40Ar/39Ar geochronologic data. Geol. Soc. Am. Bull. 133. https://doi.org/10.1130/B35560.1.
Selenka, L., Blanckenhorn, M., 1911. Die Pithecanthropus-Schichten auf Java. Geologische und Paläontologische Ergebnisse der Trinil-Expidition (1907 und 1908). W. Engelmann, Leipzig.
Sondaar, P.Y., 1984. Faunal evolution and the mammalian bio stratigraphy of Java. The early evolution of man with special Emphasis on Southeast Asia and Africa. Cour. Forsch. Inst. Senckenberg, Frankfurt am Main 69, 219–235.
Storm, P., Aziz, F., de Vos, J., Kosasih, D., Baskoro, S., Ngaliman van den Hoek Ostende, L.W., 2005. Late Pleistocene Homo sapiens in a tropical rainforest fauna in East Java. J. Hum. Evol. 49, 536–545. https://doi.org/10.1016/j.jhevol.2005.06.003.
Tankersley, K.B., Wells, D.H., 2011. Further evaluation of fluoride dating by ion selective electrode analysis. North Am. Archaeol. 32, 247–265. https://doi.org/10.2190/NA.32.3.b.
Theunissen, B., 1981. Eugène Dubois and the Ape-Man from Java. Kluwer Academic Publishers, Dordrecht.
van den Bergh, G.D., de Vos, J., Sondaar, P.Y., Aziz, F., 1996. Pleistocene zoogeographic evolution of Java (Indonesia) and glacio-eustatic sea level fluctuations: a background for the presence of *Homo*. Bulletin of the Indo-Pacific Prehistory Association 14, 7–21.
van den Bergh, G.D., de Vos, J., Sondaar, P.Y., 2001. The Late Quaternary palaeogeography of mammal evolution in the Indonesian Archipelago. Palaeogeography, Palaeoclimatology, Palaeoecology, Quaternary Environmental Change in the Indonesian Region 171, 385–408. https://doi.org/10.1016/S0031-0182(01)00255-3.
van der Geer, A.A., Lyras, G.A., Volmer, R., 2018. Insular dwarfism in canids on Java (Indonesia) and its implication for the environment of *Homo erectus* during the Early and earliest Middle Pleistocene. Palaeogeogr. Palaeoclimatol. Palaeoecol. 507, 168–179. https://doi.org/10.1016/j.palaeo.2018.07.009.
Volmer, R., van der Geer, A.A., Cabrera, P.A., Wibowo, U.P., Kurniawan, I., 2019. When did Cuon reach Java?–Reinvestigation of canid fossils from *Homo erectus* faunas. Geobios 55, 89–102. https://doi.org/10.1016/J.GEOBIOS.2019.06.004.
Westaway, K.E., Morwood, M.J., Roberts, R.G., Rokus, A.D., Zhao, J. -x., Storm, P., Aziz, F., van den Bergh, G., Hadi, P., Jatmiko de Vos, J., 2007. Age and biostratigraphic significance of the Punung rainforest fauna, East Java, Indonesia, and implications for Pongo and Homo. J. Hum. Evol. 53, 709–717. https://doi.org/10.1016/j.jhevol.2007.06.002.